Cand. Scient. Thesis in Physical Oceanography

Benguela Niños: Observations and modelling

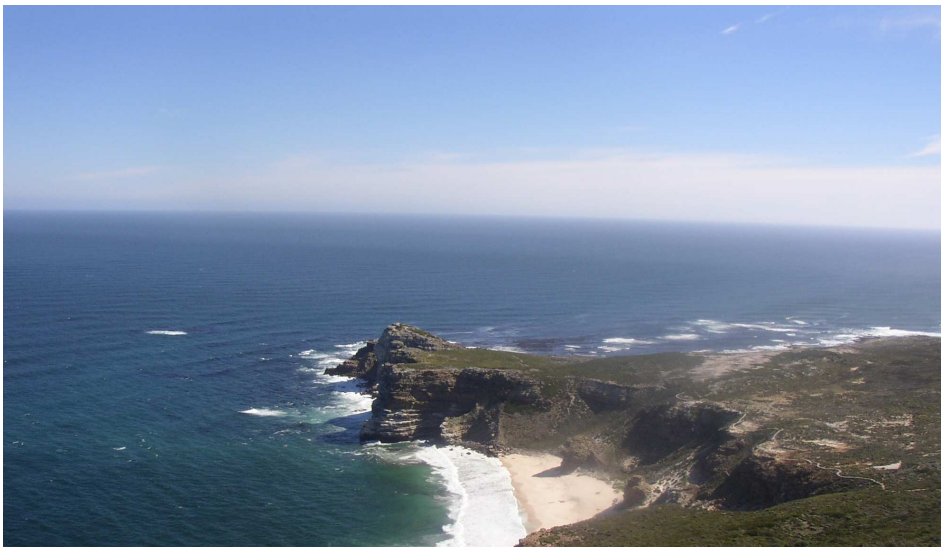

Elisabeth Hansen

April 2004

Geophysical Institute
University of Bergen

Abstract

A numerical ocean model for the South Atlantic was used to study the 1995 Benguela Niño in order to learn about the underlying forcing mechanisms of the phenomenon. By comparing observations and model output, it was found that the model WANE was unable to simulate the thermohaline signal of the 1995 event. It proved more successful at reproducing the current systems of the area. Another model simulation (OPA) was able to recreate both the surface and subsurface temperature signal of the 1984 and 1995 Benguela Niño. The main reason for the poor water mass representation during a warm event in WANE is probably the relaxation of the surface fluxes towards climatology.

An investigation of the movements of a drifter buoy and winds during the 1995 Benguela Niño revealed a strong poleward current that moved against the southerly winds, indicating that local winds are not the main driving force of the phenomenon. It is believed that the origin of Benguela Niños is found in the western part of the equatorial Atlantic; as the trade winds off the coast of Brazil weaken, this relaxation leads to the generation of equatorial Kelvin waves which propagates across the equator and poleward along the coast of Africa. The east-west component of the wind in the western equatorial Atlantic was examined, and there seems to be a relationship between the winds off Brazil and the Benguela Niños. Both numerical model simulations and the wind data support the governing theory of the generation and forcing mechanisms of Benguela Niños.

Acknowledgements

First of all I would like to express my gratitude to my advisor Tor Gammelsrød. He gave me an interesting opportunity to explore warmer waters and was an invaluable help throughout the long process. Thanks to Geir Evensen, for providing the model data and for always taking the time to answer my questions. I was fortunate enough to spend two months at the University of Cape Town in South Africa - thank you to Frank Shillington, Pierre Florenchie and everyone at the Department of Oceanography at UCT.

I would never have come this far without the help from everyone at Geofysen. Vidar Lien has been a big support and Karolina Widell and Povl Abrahamsen have assisted me with various computer problems. All the students at GFI deserve a big thank you for making this a fun place to study!

Last but not least, I would like to thank my family, Sergio and Kari for always being there for me.

Elisabeth Hansen
Bergen, March 11, 2004

Contents

Chapter 1

Introduction

The Benguela is located off the west coast of southern Africa, and is one of the four major eastern boundary current systems in the world. The oceanographic conditions in the southern Benguela are highly influenced by coastal upwelling of nutrient-rich water. Further north, warmer tropical waters dominate. The current systems and wind regimes as well as bottom topography make the Benguela a highly complex hydrographic location (Shannon & Nelson 1996).

The well-known El Niño in the Pacific has an Atlantic counterpart known as the Benguela Niño. The Benguela Niño is less intense and does not occur as often, but there are great similarities between the two when it comes to the dynamics and the underlying forcing mechanisms. The main characteristic of Benguela Niños is a strong positive temperature anomaly off the coast of Angola and Namibia during austral autumn of the year in question (Shannon et al. 1986).

The strongest and best documented Benguela Niños took place in 1963, 1984 and most recently in 1995. Common features in addition to the positive temperature anomaly in the coastal areas include negative salinity anomalies in the northern Benguela, higher than normal sea surface elevation and increased rainfall over the African continent (Shannon et al. 1986), (Gammelsrød et al. 1998), (Rouault et al. 2003).

The warm events influence the biota of the area; during the 95 Benguela Niño widespread fish mortalities were observed. The anomalous conditions also influenced the egg production and spawning, thereby affecting the local fishing industry long after the oceanographic variables had returned back to normal (Gammelsrød et al. 1998). The dynamics of Benguela Niños are not yet fully understood, and due to their climatic and economic impacts it is important to continue studying this phenomenon.

The objective of this thesis was to study the 1995 Benguela Niño by using a numerical ocean model for the South Atlantic. By studying how the model was able to describe the event, it was hoped that one would be able to further expand the knowledge of the dynamics and forcing mechanisms of Benguela Niños.

A description of the area, the phenomenon and observations during the Benguela Niños in 1963, 1984 and 1995 is given in chapter 2. The numerical ocean model WANE is described in the following chapter, while the results from the model are presented in chapter 4. Chapter

5 discusses the model findings compared to observations and results from other numerical models, while chapter 6 comprises a short summary and conclusions.

Chapter 2

Benguela Niños

2.1 The Benguela area

The Benguela area is situated off the south-western coast of Africa, between 14°S and 37°S and with a western boundary at the 0° meridian (Shannon & Nelson 1996). The ocean circulation in this area is part of the eastern boundary current system of the South Atlantic. The Benguela oceanography is dominated by a coastal upwelling system, just like the other major eastern boundary current regions of the world. These are found off California, north-west Africa and Peru. The Benguela is unique in that it is bounded by warm water regimes at both the northern and southern boundary (Shannon & Nelson 1996). A map of the bottom topography off Angola and Namibia is shown in figure 2.1.

Water masses

The surface water in the Benguela is according to O'Toole (1980) comprised of three distinct water masses. Cold, low-salinity (34.9–35.2 psu) surface water from the upwelling region is mainly found in the southern region. Temperatures range between 12°C and 16°C. Between 19°S and 22°S a mixed water mass of moderate salinity (35.2–35.5 psu) and temperature (16–20°C) is found. Further north, a warm, high-salinity (17–22°C and 35.5–35.9 psu) water mass periodically advances southwards from Angolan waters and retreats to the north-west (O'Toole 1980).

Current systems

The ocean circulation off the Angolan and Namibian coast is maintained by two major current systems. The southerly influence is comprised of several branches of the South Equatorial Current as well as the Benguela Current, a mainly wind-driven current which flows along the coast from the southern tip of the African continent. Eastward-flowing currents of equatorial origin enter the system from the north; the Equatorial Undercurrent (EUC), the South Equatorial Countercurrent (SECC) and the South Equatorial Undercurrent (SEUC) are deflected at the coast of Africa and feed the Gabon Current, which continues poleward as the Angola Current (AC). The surface component of the Angola Current is diverted towards the west at

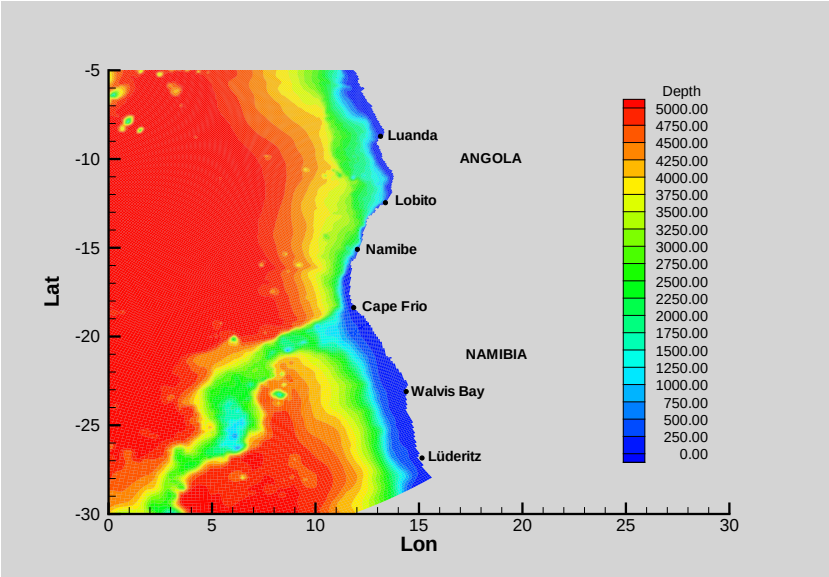

Figure 2.1: *Map of the coastal areas of Angola and Namibia with bottom topography.*

about 15–19°S and recirculates equatorward at about 1°W (Mohrholz et al. 2001).

Wind patterns

The wind patterns in the Benguela are strongly influenced by the anticyclonic motion around the semi-permanent high pressure system over the South Atlantic, as well as the seasonal low pressure system that develops over the subcontinent during austral summer. The predominant winds in the area are from the south and southeast (Shannon & Nelson 1996).

Benguela upwelling

The southerly and south-easterly winds in the Benguela region drive an offshore surface drift which leads to coastal upwelling of nutrient-rich, cold water. There are a number of upwelling cells along the southwestern coast of Africa from Cape Point (34.35°S) to Cape Frio (18.4°S) (Peterson & Stramma 1991). The main semi-permanent upwelling cell is near Lüderitz (27°S) (Shannon & Nelson 1996).

The Angola-Benguela Frontal Zone

The Benguela's northern boundary is the Angola-Benguela Frontal Zone (ABFZ), which separates the cold, upwelled water in the Benguela from the warm, tropical Angola Current water. The ABFZ migrates seasonally, and the average position of its northern boundary moves between 14°S in August and 17°S in March (Meeuwis & Lutjeharms 1990). The southern boundary of the ABFZ normally does not move further south than 22°S (Mohrholz et al. 2001).

The front is aligned perpendicular to the coast, with a seaward extension of between 200 and 600 km. Its average width is approximately 200 km. There are strong horizontal gradients in both temperature and salinity in the upper 50 m, but the front can be identified to a depth of at least 200 m. The Angola-Benguela frontal zone is a complicated system, with multiple eddies, meanders and filaments which cause great temporal and spatial variability (Lass et al. 2000). The location and composition of the frontal zone is sensitive to local wind stress, and its position may shift rapidly (Mohrholz et al. 2001).

2.2 Theory

2.2.1 El Niños

The term El Niño refers to a climatic event in the Pacific, which usually takes place every 2–10 years. Originally, the name El Niño (the Christ child) was the local name for the annual increase in the sea temperature off Ecuador and Peru around Christmas time. During this period there is a southward flow of warm water along the coast due to a relaxation of upwelling or a depression of the seasonal thermocline (Tomczak & Godfrey 2003). Some years there is an anomalous amount of warm water covering the Pacific, and these events are now known as El Niños.

Prior to an El Niño event there is a weakening of the South East trade winds in the western part of the ocean basin. This leads to a collapse in the sea surface slope, and the thermocline becomes nearly horizontal. This enables warm water to move eastwards across the ocean. In the western Pacific the weakening of the trade winds occurs abruptly, generating equatorial Kelvin waves that move along the equator. As the Kelvin waves reach the eastern part of the basin and hit land, they are split into northward- and southward-travelling coastal Kelvin waves which propagate the anomalies along the coast (Bearman et al. 1998). There is an increase in sea level as water piles up along the coast, as well as a deepening of the thermocline.

2.2.2 Benguela Niños

There have been several documented warm events in the Atlantic ocean, and because of the similarity to the El Niño phenomenon they have been termed Benguela Niños (Shannon et al. 1986). They are generally observed as intrusions of warm, saline water along the south-western coast of Africa. This surface intrusion is believed to be of equatorial origin, and it propagates poleward along the coast as far south as 25°S. Benguela Niños are less intense and less frequent than their Pacific counterparts (Gammelsrød et al. 1998). It is thought that the origin of these events is found in the western part of the equatorial Atlantic; as the trade winds off the coast of Brazil weaken, this relaxation leads to the generation of equatorial Kelvin waves as well as a strengthening of the South Equatorial Counter Current (SECC). This produces a depression of the thermocline along the equator (Rouault et al. 2003).

The major warm events known as Benguela Niños share a number of characteristics. During Benguela Niños anomalously high sea surface temperatures (SST) have been observed

for at least six months or longer. During the last two Benguela Niños the equatorward wind-stress over the northern part of the Benguela was stronger than normal, but still a poleward intrusion of warm, saline water suppressed the upwelling. The average sea level was higher than normal for at least a year, with maximum values coinciding with the maximum SST. The events were accompanied by high rainfall over Namibia (Shannon et al. 1986).

2.3 Observations

2.3.1 Previous Benguela Niños

The first documented climatic event in the Benguela occurred in 1933/34. Observations showed that the SST near Walvis Bay between March and July 1934 were 2–3°C above the 15 year monthly mean values (Shannon et al. 1986). Although several warm events have been recorded since then, some of the strongest and best documented took place in 1963 and 1984. The 1995 Benguela Niño will be described in a separate section.

The 1963 Benguela Niño

Observations from ten stations in the central Namibian area in 1963 reveal that salinity and temperature near Walvis Bay were anomalously high in the upper 50 meters during the austral fall, and the highest mean values were reached in June, with a maximum temperature of 18°C. The maximum recorded temperature anomaly was 5°C (Shannon et al. 1986).

Late 1963 SST data from the St. Helena Bay area (32–33°S) and Cape Town shows a positive temperature anomaly of about 2°C in the southern Benguela. Although the strongest signal is usually found further north, the fact that the 1963 Benguela Niño was felt this far south suggests that is was a strong event (Shannon et al. 1986).

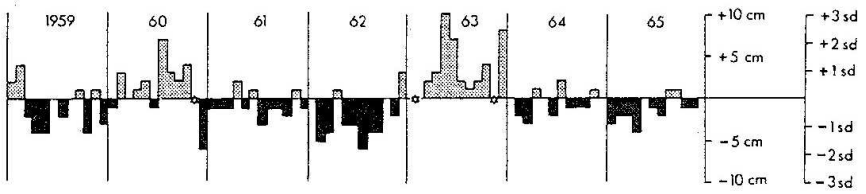

Figure 2.2: *Anomalies in the pressure adjusted mean monthly sea level at Walvis Bay from 1959 to 1965. From Shannon et al. 1986.*

There was unusually high rainfall over much of the Namib desert in 1963; in January to April the values were typically double the average.

The Benguela Niño is characterized by temperature and salinity anomalies seen at and below the surface during austral autumn. The thermohaline signal is accompanied by changes in the sea surface height (SSH). Measurements of the sea level near Walvis Bay from 1959 to 1965 show anomalous conditions in 1963 (see figure 2.2); following two years of negative pressure adjusted sea level anomalies in 1961 and 1962, a positive anomaly lasted throughout 1963 with a maximum in March 1963 (Shannon et al. 1986).

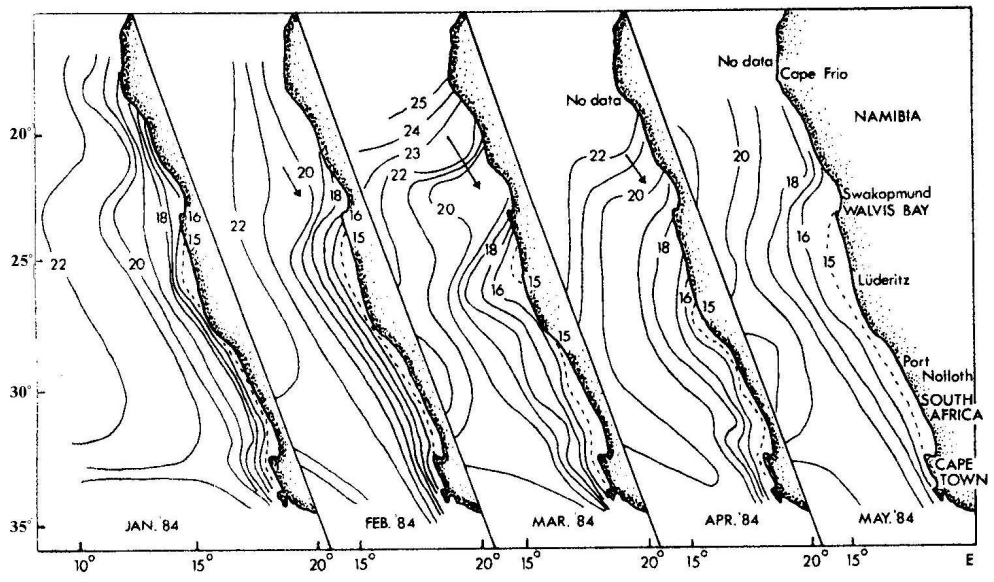

Figure 2.3: *SST from January to May 1984 from S.A. Weather Bureau. From Shannon and Boyd (1986).*

Other observations that confirm the existence of a 1963 Benguela Niño are summarized in Shannon et al. (1986).

The 1984 Benguela Niño

Figure 2.3 shows the distribution of SST in the Benguela region between January and May 1984 in the coastal regions of the south-western Africa. The data, which are from the S.A. Weather Bureau, show an intrusion of warm water from the north or northwest with a maximum in March and April. A research cruise in March 1984 provided more accurate data for the Namibian coast. Temperature and salinity anomalies were typically +6°C and +0.6 psu for the area north of 23°S, and the warm, saline Angolan water penetrated at least as far south as 25°S. The temperature and salinity at 50 m were also higher than normal, with typical values of 2°C and 0.2 psu. The intrusion of warm and saline water penetrated about 5°further south than normal during the late summer and early fall of 1984, and suppressed upwelling in the northern Benguela (Shannon et al. 1986).

The fact that this intrusion occurred although the equatorward wind stress in the same area was stronger than normal suggests that the forcing mechanisms of the Benguela Niños are related to large scale wind patterns rather than local winds (Shannon et al. 1986).

As in 1963, the rainfall over Namibia in 1984 was well above average. There is also evidence of changes in sea level during the 1984 Benguela Niño, as can be seen in figure 2.4. The sea level near Walvis Bay was lower than normal throughout 1982 and the first 9 months of 1983, while there was a positive anomaly in October 1983. This persisted through 1984, with a temporary decline in April and May. The maximum sea level values were recorded

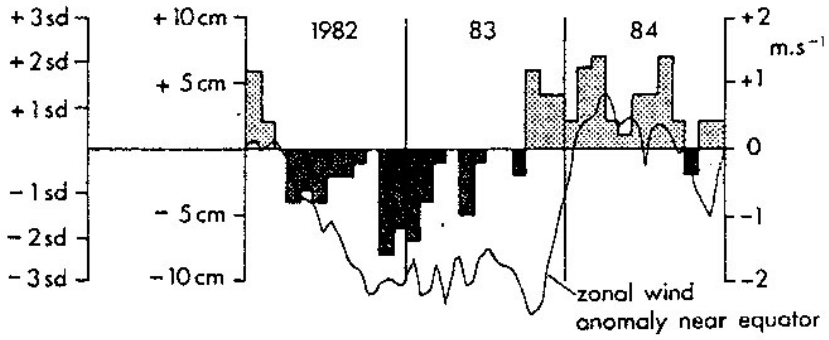

Figure 2.4: *Anomalies in the pressure adjusted mean monthly sea level at Walvis Bay from 1982 to 1984. From Shannon et al. 1986.*

in March 1984. The pressure adjusted sea level anomaly from 1982 to 1984 follows the same pattern as that from 1961 to 1963 (Shannon et al. 1986).

2.3.2 The 1995 Benguela Niño

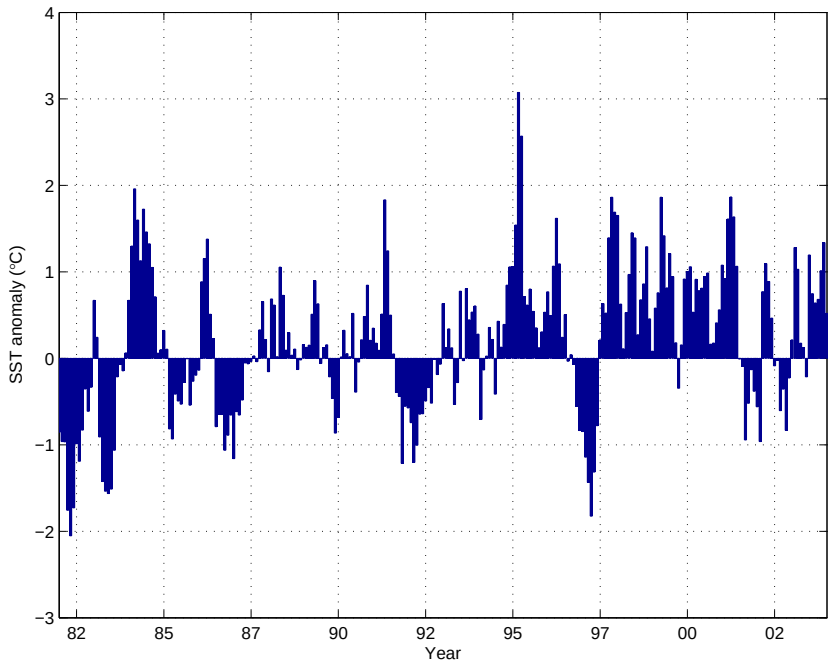

Figure 2.5: *OI-SST monthly averages of temperature anomaly averaged over 20–10° S and 8–15° E. From NOAA Climate Prediction Center.*

Figure 2.5 shows SST anomalies calculated from the NOAA Optimal Interpolated Sea Surface Temperature (OI-SST) analysis. It is a combination of satellite and in situ data, and

has a resolution of 1 degree (Reynolds & Smith 1994). The time series is from 1982 to 2002 and the data are averaged over 20–10°S, 8–15°E. The figure shows a positive temperature anomaly in 1984; this is the 1984 Benguela Niño. There is also a strong temperature anomaly in 1995, which suggests a warm event in 1995 as well.

The 1995 Benguela Niño coincided with two parallel research cruises in late February and early March 1995. The research vessels *Dr Fridtjof Nansen* and *Welwitchia* conducted surveys in Angolan and Namibian waters respectively. During these cruises several measurements were taken, and the results are published in Gammelsrød et al. (1998).

Temperature

The maximum temperature anomalies during the 1995 Benguela Niño were found below the surface layer, at a depth of about 20 meters. A vertical section perpendicular to the coast taken just south of Luanda revealed that the maximum temperature difference (> 6°C), obtained when comparing measurements from March 1994 and 1995, was found between 20 to 40 meters. In Namibian waters, a comparison between the temperature at 30 meters depth between March 1995 and 1996 revealed an anomaly of more than 8°C at 18–19°S. The mean temperature in March 1995 measured near Swakopmund in Namibia (22.5°S) was the highest since the 1984 Benguela Niño (Gammelsrød et al. 1998).

Salinity

In Angolan waters, the measurements from March 1995 compared with 1994 revealed a negative salinity anomaly with a maximum amplitude of -4 psu. This anomaly was restricted to the upper 50 meters. Negative salinity anomalies were seen along the coast as far south as Cape Frio. The negative salinity anomaly in Angolan surface waters was believed to be caused by a southward displacement of freshwater from the Congo River. In Namibian waters, a positive anomaly was detected. The longshore vertical structure from March 1995 and 1996 shows a positive salinity anomaly of 0.5 psu in the same area as the maximum temperature anomaly, at about 19°S (Gammelsrød et al. 1998).

Sea Surface Height

Figure 2.6 shows the sea surface height anomaly measured by satellites from October 1992 to October 1997 at 12.8°S, 12.8°E. It shows positive SSH anomalies of up to 20 cm during the first 4 months of 1995. This was preceded by negative anomalies during the last months of 1994 (Kvaleberg 2000).

Dynamics

Seven satellite-tracked surface drogues with a sail depth of approximately 1 meter were deployed outside the Namibian coast during the research cruise in 1995. The drifter data were provided by the South African Council for Scientific and Industrial Research and were used with permission from the National Petroleum Corporation of Namibia (NAMCOR). Figure 2.7 shows the drift path of the drogue that was deployed closest to shore near Walvis Bay.

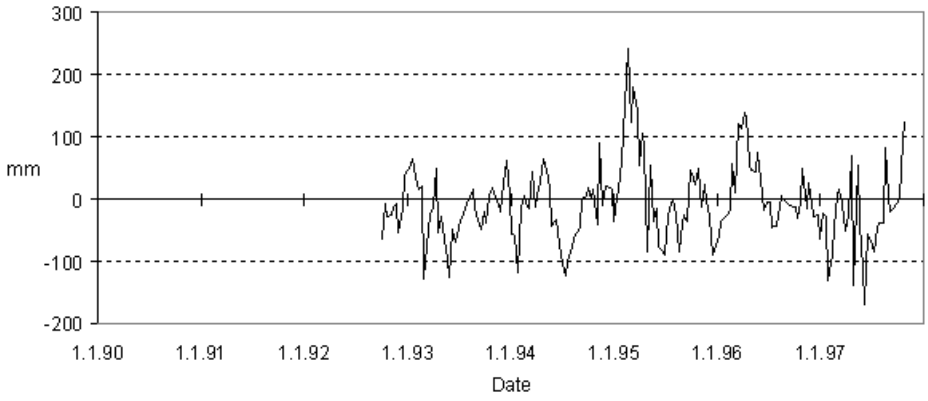

Figure 2.6: *SSH anomaly from satellite altimetry from 1993 to 1997 at 12.8S 12.8E.*

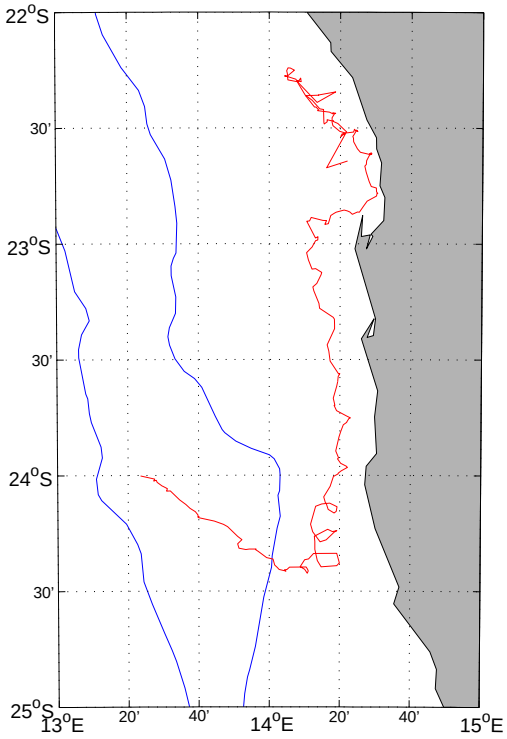

Figure 2.7: *The drift path of a surface drogue from 6/2/95 to 8/3/95.*

The drogue initially moved north-westwards, before it changed direction and started moving southwards. Near the end of the experiment the drift path shifted back to a north-westerly direction. The average speed of the surface drogue was 27 cm/s (Gammelsrød et al. 1998).

In order to find out more about how local wind might have affected the drifter's movement, we look at wind data from two different sources and make a comparison with the drifter.

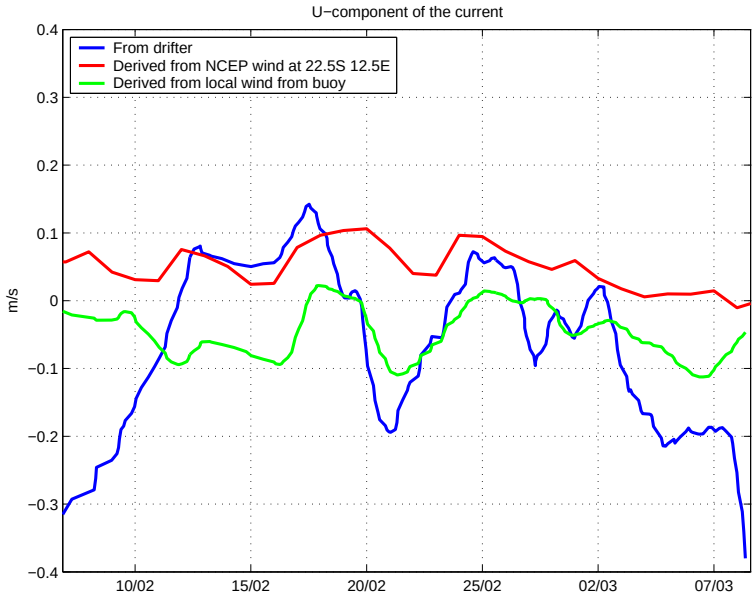

(a)

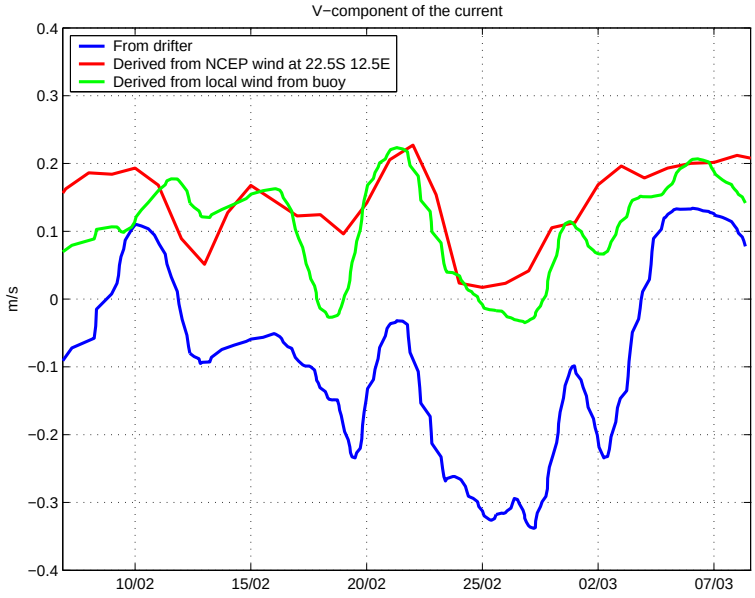

(b)

Figure 2.8: *U- and V-components of the current calculated from the drifter's movement, daily wind data from NCEP and local wind data from the drifter.*

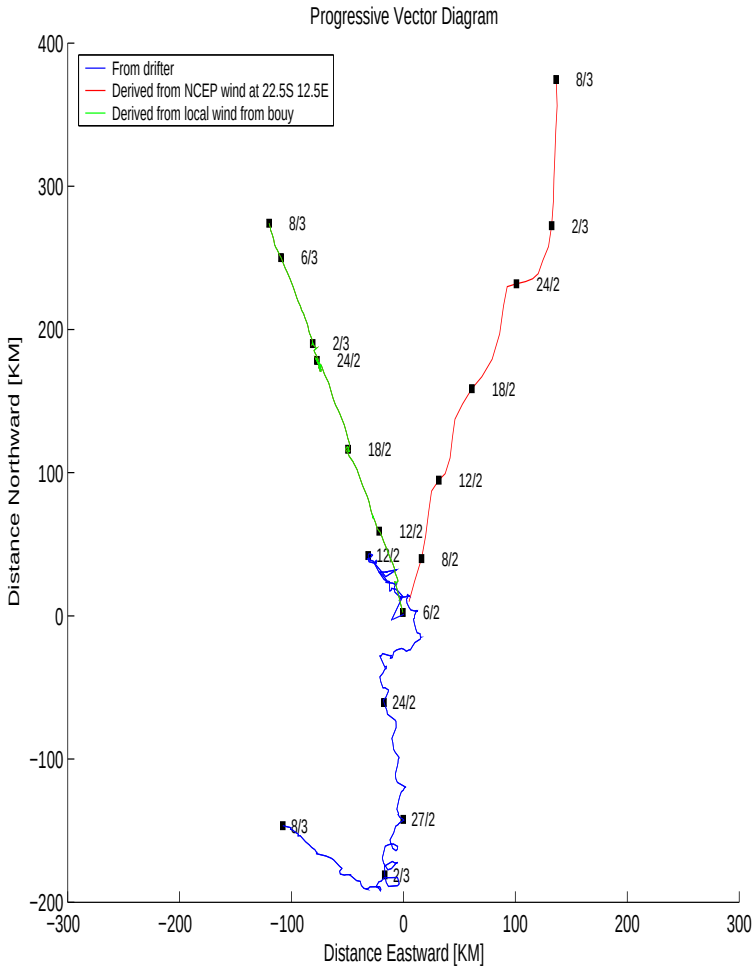

Figure 2.9: *The progressive vectors for the drifter, NCEP wind and local wind.*

Figure 2.8 shows the u- and v-component (u=east-west, v=north-south) of the current. It displays 3 different variables. The blue line shows the u- and v-components of the current, calculated from the drift path of the drogue. The red line shows components of NCEP wind at 22.5°S 12.5°E during the time the surface drogue was deployed. The wind has been scaled to be comparable to the current in figure 2.8 by plotting 2% of the actual wind. NCEP Reanalysis data were provided by the NOAA-CIRES Climate Diagnostics Center, Boulder, Colorado, USA, from their Web site at http://www.cdc.noaa.gov/. The green line shows wind measurements from a wind gauge mounted at the drifter. The local wind data has been scaled the same way as the NCEP data.

The east-west movement is shown in figure 2.8(a). There seems to be a discrepancy between the NCEP wind and the local wind; the former indicates a westerly wind, while the latter shows wind from the east. The drifter seems to be moving rather quickly in a westerly direction in the beginning and end of the time period, despite weak or positive winds. Apart from that, the drifter seems to be following the east-west component of the wind from both

NCEP and the local buoy measurements.

The v-components of the wind data sets reveal a better correlation between the two; both the local wind and the NCEP wind indicate southerly winds. The drifter, however, is moving towards the south through most of the time period. The drifter is moving in a northerly direction in the beginning and the end of the deployment period, but the main trend is southward movement. This means that the drifter is moving against the wind; despite the prevailing winds from south to north, the drifter is moving towards the south. When the winds are strong, the drifter slows down, while it speeds up when the winds weaken. This is an indication of a strong, poleward current that is moving independently from the local winds.

A plot of the progressive vector for the drifter, the NCEP wind and the local wind reveals the same pattern. This is shown in figure 2.9.

The surface drogue changed direction towards the northwest around the 3rd of March, and this is believed to day of the southernmost penetration of the 1995 Benguela Niño. All the seven drifters increased in speed and started moving in a northwestwardly direction on this day (Gammelsrød et al. 1998).

Chapter 3

Numerical Model Description

WANE (West African Normals and Extremes) is a numerical ocean model developed by Geir Evensen, formerly at the Nansen Environmental and Remote Sensing Center (NERSC) in Bergen, Norway. The WANE hindcast study has produced a modelled data set of currents, temperature and salinity for the 15-year period 1985–1999. The model covers the South Atlantic, but has enhanced resolution along the West African coast (Evensen et al. 2002).

3.1 HYCOM and MICOM

WANE is a version of the Hybrid Coordinate Ocean Model (HYCOM), a primitive equation ocean general circulation model that evolved from the Miami Isopycnic Coordinate Model (MICOM) (Bleck 2002). HYCOM was developed as a result of collaborative efforts between the University of Miami, the Los Alamos National Laboratory and the Naval Research Institute, and the main objective was to address known shortcomings of the MICOM vertical discretization scheme (Halliwell 2001).

Vertical coordinates

There are different ways to treat the vertical stratification of water in numerical models. Isopycnal models use Lagrangian movement; a coordinate surface is moving with the water in the vertical. In models with a fixed vertical coordinate system, e.g. z-level and sigma-coordinate models, the water moves through the coordinate surface (Evensen et al. 2002). The isopycnic coordinate enables the model to retain its water mass characteristics for centuries of integration, while the z-level coordinate model gives the possibility to obtain a high vertical resolution in the surface mixed layer. Models using the terrain-following sigma coordinate maintain sufficient vertical resolution in unstratified or weakly-stratified regions and have high vertical resolution in coastal regions (Evensen et al. 2002).

MICOM uses potential density as the vertical coordinate for all but the surface layer, which is treated as a bulk mixed layer with variable temperature and salinity (Evensen et al. 2002). MICOM has produced good scientific results, but the representation of vertical mixing and oceanic flow in shallow-water and weakly stratified regions are constrained by the limitations in the vertical coordinate (Halliwell 2001).

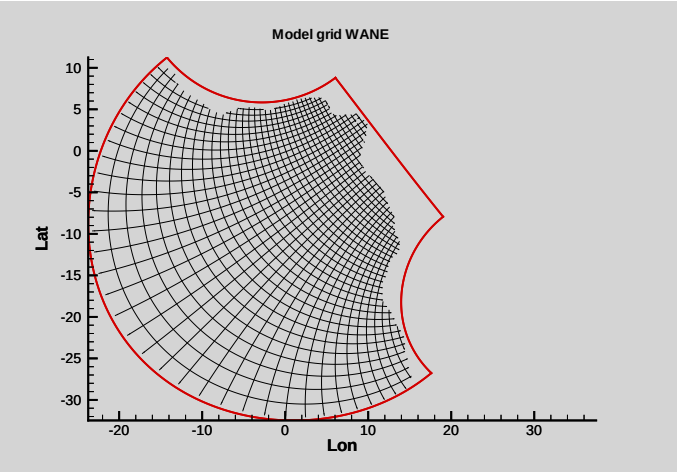

Figure 3.1: *The WANE model grid*

HYCOM uses the hybrid coordinate. The hybrid coordinate is isopycnal in the open, stratified ocean, but smoothly reverts to a terrain-following coordinate in shallow coastal regions. In the mixed layer and/or unstratified seas, a z-level coordinate is used (Evensen et al. 2002). The hybrid coordinate extends the geographic range of applicability of traditional isopycnic coordinate models, such as MICOM, toward shallow coastal seas and unstratified parts of the ocean (Evensen et al. 2002).

The HYCOM model algorithm for vertical discretization assigns a reference isopycnal to each layer. For all layers except the bottom layers intersecting topography, a minimum thickness is defined. Should water with a specific reference density cease to exist in the vertical water column, the isopycnal layer might approach its minimum thickness. If so, this layer is used as a vertical level coordinate, and this results in better resolution in the mixed layer (Evensen et al. 2002). The position of the level coordinate is predefined in the model to avoid crowding of coordinate surfaces (Halliwell 2002).

3.2 WANE setup

Model grid

The model grid in WANE covers most of the South Atlantic, with enhanced resolution along the west coast of Africa. The resolution of the WANE model grid is 5–6 km along the West African coast and up to 20 km in the open sea.

The WANE model grid, shown in figure 3.1, has 350 times 373 grid points in the horizontal and 13 layers in the vertical. The model uses the isopycnal coordinate in the open, stratified seas and the z-level coordinate in the mixed layer and unstratified seas (Evensen et al. 2002).

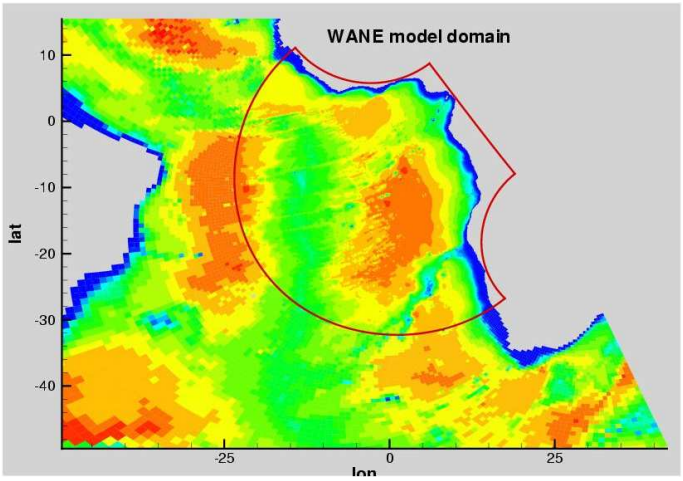

Figure 3.2: *South Atlantic bathymetry in the coarse WAX grid. The WANE grid is marked by the red frame.*

Boundary conditions and initialization

The boundary conditions for WANE are obtained by using data from a large-scale, coarser model. Figure 3.2 shows the WANE model domain nested into the larger model domain of the WAX model (Evensen 1998). Using a one-way nesting scheme, the boundary conditions from the regional model (WANE) are relaxed towards the output from the coarser model. This is the case for the slowly varying variables, such as temperature, salinity, baroclinic velocities and layer interfaces. For the barotropic variables, a more complex scheme is used in order to avoid reflection of waves at the model boundaries (Evensen et al. 2002).

Because the initialization of the regional model is based on interpolation from the model output generated in the WAX model, only a short adjustment integration was needed to get the fields in proper dynamical balance (Evensen et al. 2002).

Climatology

The surface fluxes of heat and freshwater in WANE are relaxed towards the Levitus climatology. The timescale for relaxation towards the climatological data is 47 days for temperature and salinity. In theory that means that after an integration period of 47 days, the temperature and salinity will be a factor of 1/e (1/2.72) closer to the Levitus data, in the idealized case with no influence from dynamical processes.

Bathymetry and tides

The data set used for initializing the bathymetry of the regional and the coarser model was an extended version of ETOPO5 called DS759.2, with a resolution of 5 minutes (Evensen et al. 2002). The University of Texas provided the UT/CSR data set, which is used for specifying the tides (Evensen et al. 2002).

Atmospheric wind data

The wind data was provided by Oceanweather Inc, who reanalyzed the original data set from NCEP. The data set gives the wind every 6 hours with a resolution of 0.62 degrees.

River fluxes

The river fluxes were computed using data from the Max Planck Institute in Hamburg. Freshwater fluxes from the Niger and the Congo River are included in the model. The data used are monthly averaged climatologies derived from multiyear time series of river discharges (Dümenil et al. 1993).

Model integration

The model was integrated for the time period from 1985 to 1999, and a 15 years data set was produced. Weekly averages of all model fields were stored. The model was integrated using a multi processor Cray Origin 2000, using 20 CPUs continuously for close to 5 months (Evensen et al. 2002).

Chapter 4

Results

In this section selected output from the model WANE is presented. The model data are visualized using software developed by Amtec. The program is called Tecplot (version 7.5), and it makes it possible to show the model data in a number of different representations.

The data are presented in horizontal and vertical sections, and they are shown as weekly, monthly or yearly averages.

4.1 Horizontal sections

The horizontal sections from the WANE model show the different variables at the layer interface. The values shown in each layer is an average of the layer below the interface; a horizontal section showing layer 1 gives the mean values for the upper 10 meters. An example is shown in figure 4.1, which shows the temperature in the upper layer for a yearly average of 1995.

The boundary of the vertical layers is determined by the density, as described in chapter 2. Thus the boundary of each layer follows the density interfaces, and the vertical position of a specific point could be very different from another point in the same plot.

4.1.1 Monthly means

To illustrate the general development of the oceanic conditions in the Benguela area through the year, selected figures of the monthly means through 15 years are presented. The monthly means are computed by averaging the data from a certain month from 1985 to 1999.

Temperature

In austral autumn the sea surface temperature is at its maximum. Figure 4.2 shows the monthly averaged temperature in March, June, September and December for layer 1 along the south-western coast of Africa. Figure 4.2(a) shows the SST in March. The temperature in the upper layer decreases from north to south, and the isolines are generally nearly perpendicular to the coast. The temperature is close to 28°C in the northern part of the section, with decreasing temperatures towards the south. In the far south of the section, the temperature

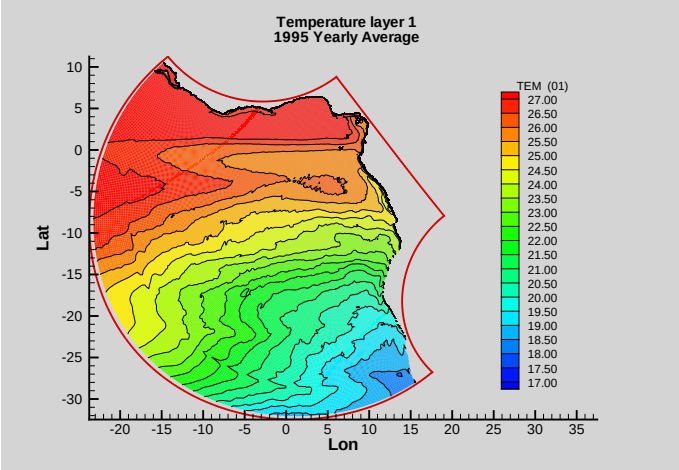

Figure 4.1: *Temperature in the upper layer, 1995 average.*

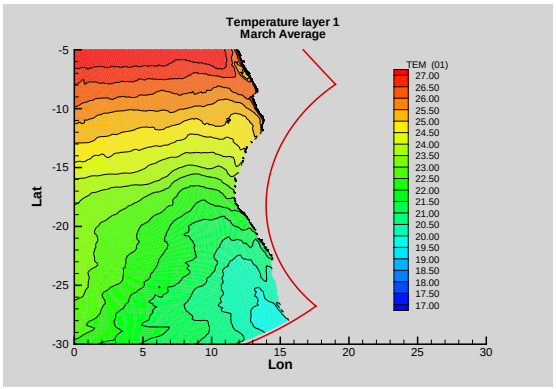

(a) March

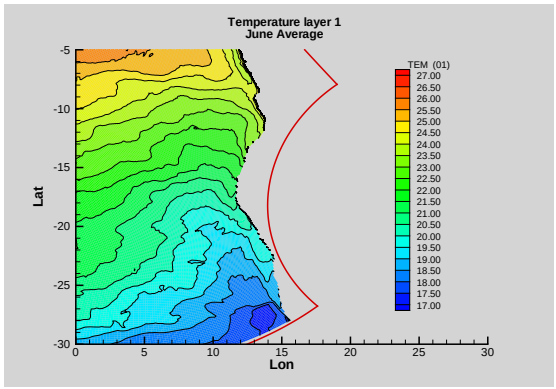

(b) June

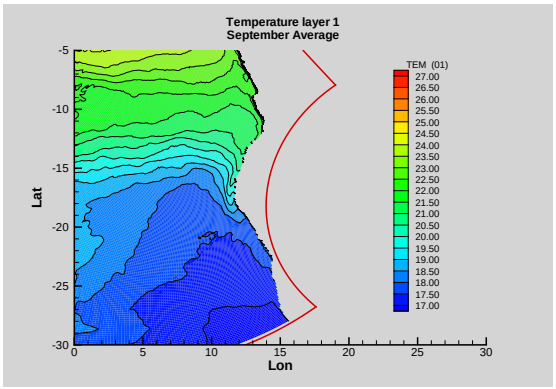

(c) September

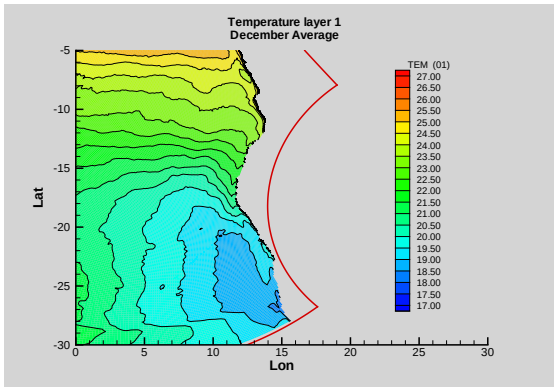

(d) December

Figure 4.2: *Monthly average temperature in layer 1 for March, June, September and December*

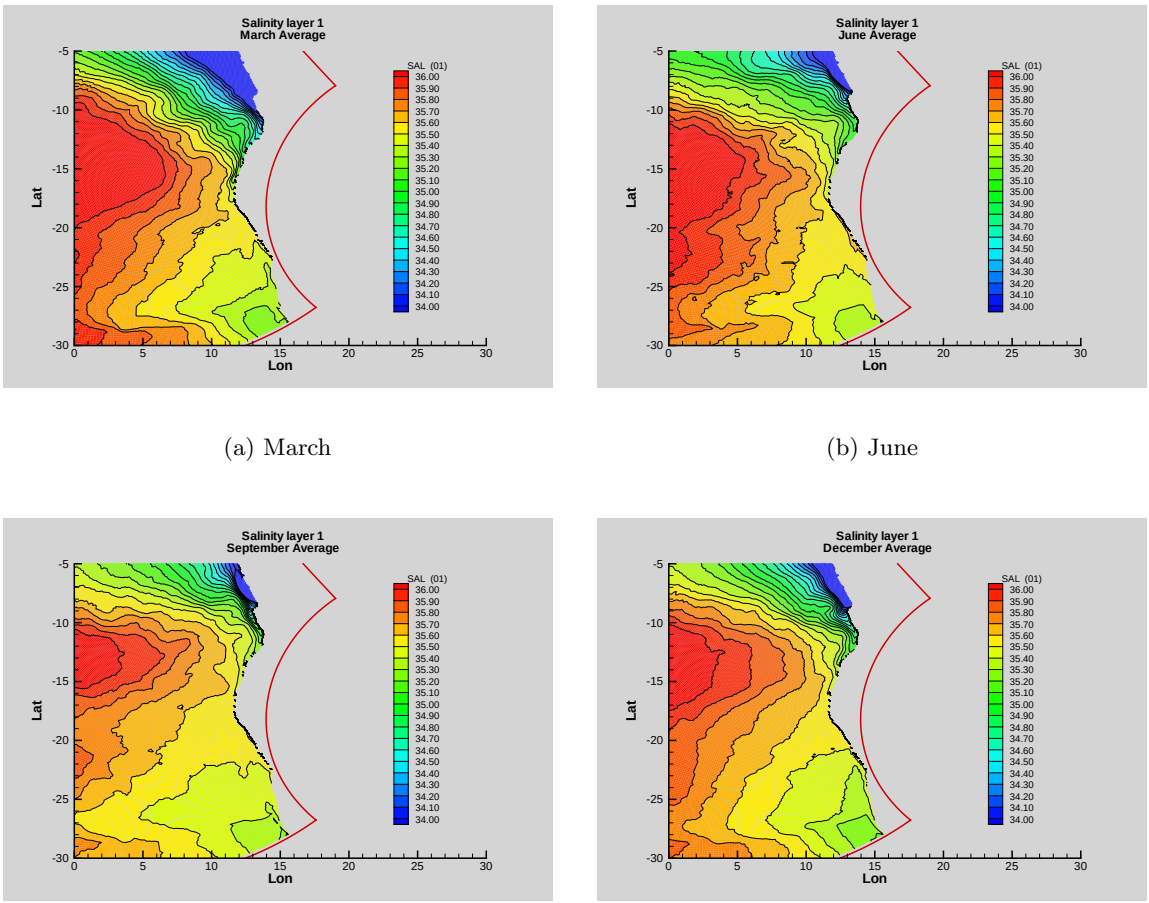

(a) March

(b) June

(c) September

(d) December

Figure 4.3: *Monthly average salinity in layer 1 for March, June, September and December*

is around 20°C. This relatively low temperature is caused by upwelling of cold, low-saline water in the southern Benguela. The Angola-Benguela front, which is usually found between 14 and 17°S, is according to the model weak in this month.

In June (figure 4.2(b)) the surface water in the entire area is colder. The highest temperature in the north is around 25°C, while the southern minimum is just above 17°C. This trend continues throughout the austral winter and early spring, and in September (figure 4.2(c)) the maximum temperature in the north is less than 24°. The cold water from the south now extends further north, and there is a marked front around 13–17°S. The temperature in the southern Benguela is below 17°C. As summers returns, the surface temperature increases again, and in December (figure 4.2(d)) surface waters with temperatures over 25°C is seen around 5°S. The lowest temperature observed in the upwelling area in the south is just below 19°C. The frontal zone is still visible, but not as pronounced as in September.

Salinity

A similar development is seen in the plots of salinity in the upper layer (figure 4.3). The outflow from the Congo River is clearly visible between 5–10°S. The river outflow affects a large area in Angolan waters, and during the period of maximum extent water with salinity lower than 34 psu can be seen as far offshore as 9°E. The low-salinity river outflow reaches its maximum extent in austral fall (March/April), as can be seen in figure 4.3(a). A tongue of low-salinity water along the coast can be seen between 12°S and 17°S. There is also a local salinity minimum in the Benguela upwelling area near the southernmost limit, between 25 and 30°S. The minimum salinity near the coast is just below 35.3 psu. More saline surface ($>$ 36 psu) water is found in the open sea, with decreasing values as we get closer to the coast.

The salinity plot for June (figure 4.3(b)) shows that the low-salinity river outflow has a smaller westward extent than in March. In the southern Benguela the water is slightly more saline, with minimum values just below 35.4 psu. In September (figure 4.3(c)), the river outflow seems to be more confined to coastal areas, while the salinity in the upwelling area remains the same. The high-salinity water in the open sea has moved further offshore. December (figure 4.3(d)) brings a stronger westward extent of the river outflow and slightly less saline Benguela water.

4.1.2 The 1995 Benguela Niño

The strongest signal of the 1995 Benguela Niño was observed in March. The main focus will therefore be on this month, and using the averaged monthly means as a reference we will try to discover signs of the warm event in the model.

Temperature

Figure 4.4 shows the temperature in March 1995 for the 4 top layers. The top layer is the upper 10 meters, while the second is usually found between 10 and 20 meters. The depth of the deeper layers is more variable, depending on the density and proximity to land. However, in general the third layer is located between 20–50 meters, and layer 4 is found between 50–100 meters.

The general picture in the surface layer is similar to that presented in the monthly mean for March. The plots from layers 2, 3 and 4 show that the temperature decreases with depth. A marked frontal zone is not easily identified. The surface temperature ranges from 28°C in the north to just below 19°C in the Benguela upwelling area. Note that the temperature close to shore between 15°and 20°S is 22–25°C in the surface layer, and slightly lower in the subsurface layers.

Temperature anomalies for the different layers are plotted by subtracting the temperature values of the month/week we want to look at from the model monthly mean and plotting the difference. Figure 4.5 shows the temperature anomaly for March 1995 for the three upper layers. In layer 1 (figure 4.5(a)) a positive anomaly can be seen around 6°S, with a maximum

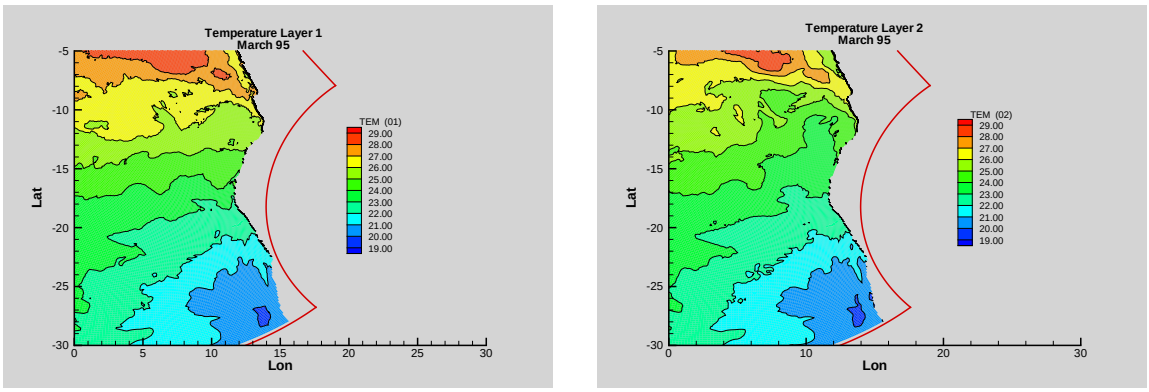

(a) Layer 1

(b) Layer 2

(c) Layer 3

(d) Layer 4

Figure 4.4: *Temperature for March 1995 in layers 1-4*

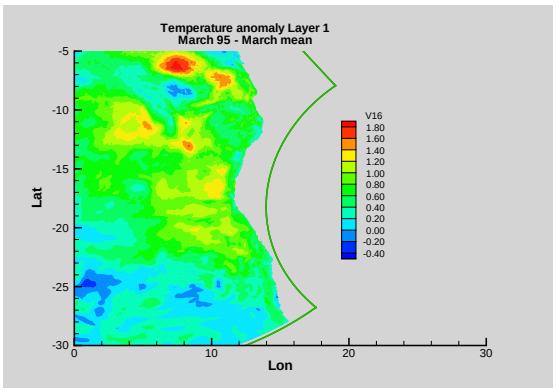

(a) Layer 1

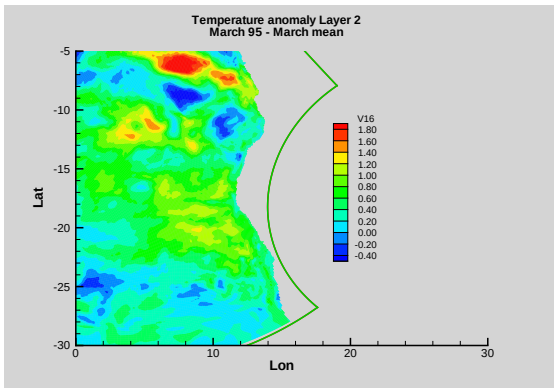

(b) Layer 2

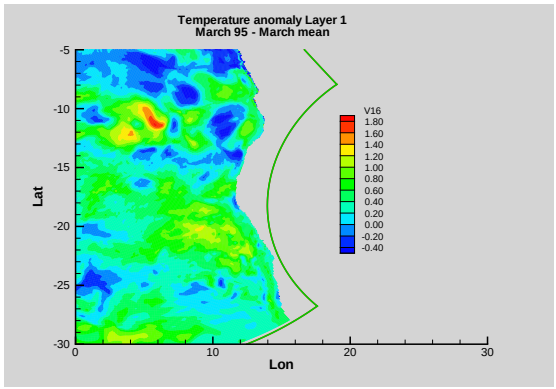

(c) Layer 3

Figure 4.5: *Temperature anomalies for March 95, layers 1, 2 and 3.*

value of 1.8°C. It has the shape of an ellipsoid, and extends over 2°of latitude and longitude. Patches of positive anomalies can be seen in the area north of 25°S, with values up to 1.5°C.

In layer 2 (figure 4.5(b)) the positive anomaly in Angolan waters (6°S) is stronger; the temperature difference between March 95 and the March mean reaches 2°C. A weak negative anomaly is seen just south of that. The general picture remains similar to that seen in layer 1.

Layer 3, shown in figure 4.5(c), displays mostly negative temperature anomalies of up to 0.4°C. The area of weak positive anomalies seen in the upper two layers between 15 and 20°S is still visible, but weaker in this layer. An area of negative temperature anomalies is seen close to Cape Frio (18°S).

Salinity

The salinity plots for the 4 upper layers are shown in figure 4.6. The decreasing influence of the freshwater from the Congo River with depth is clear; in layer 4 only a narrow area

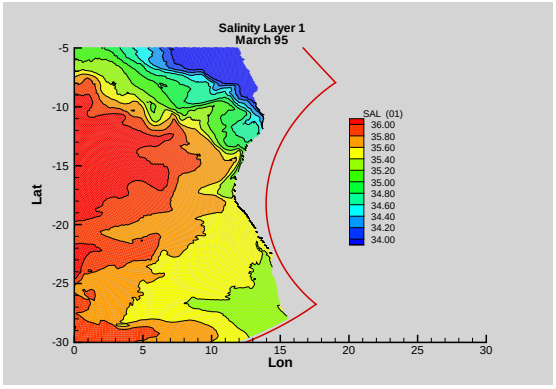

(a) Layer 1

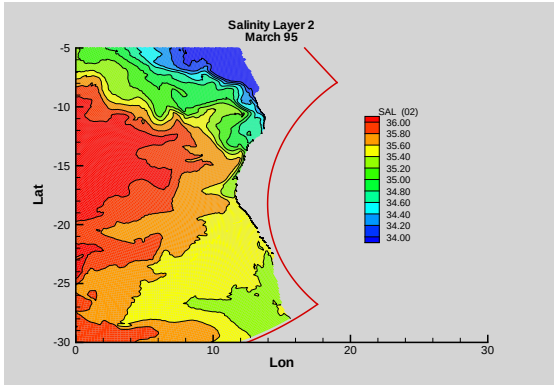

(b) Layer 2

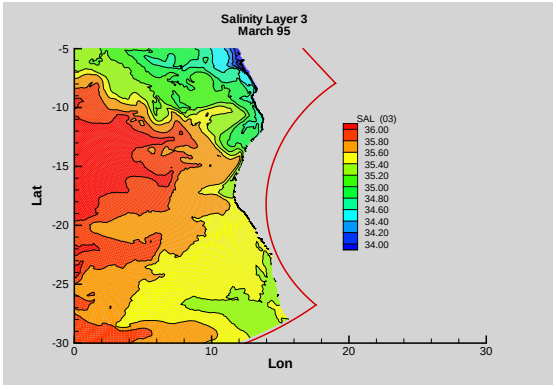

(c) Layer 3

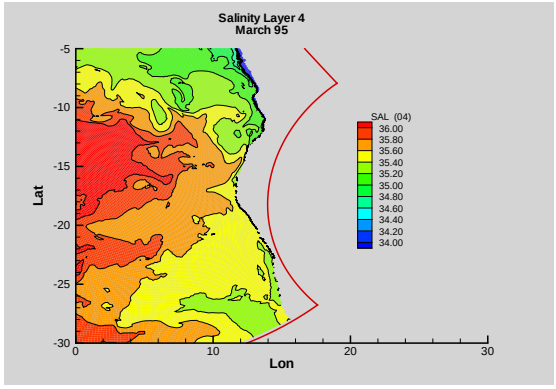

(d) Layer 4

Figure 4.6: *Salinity for March 1995 in layers 1-4*

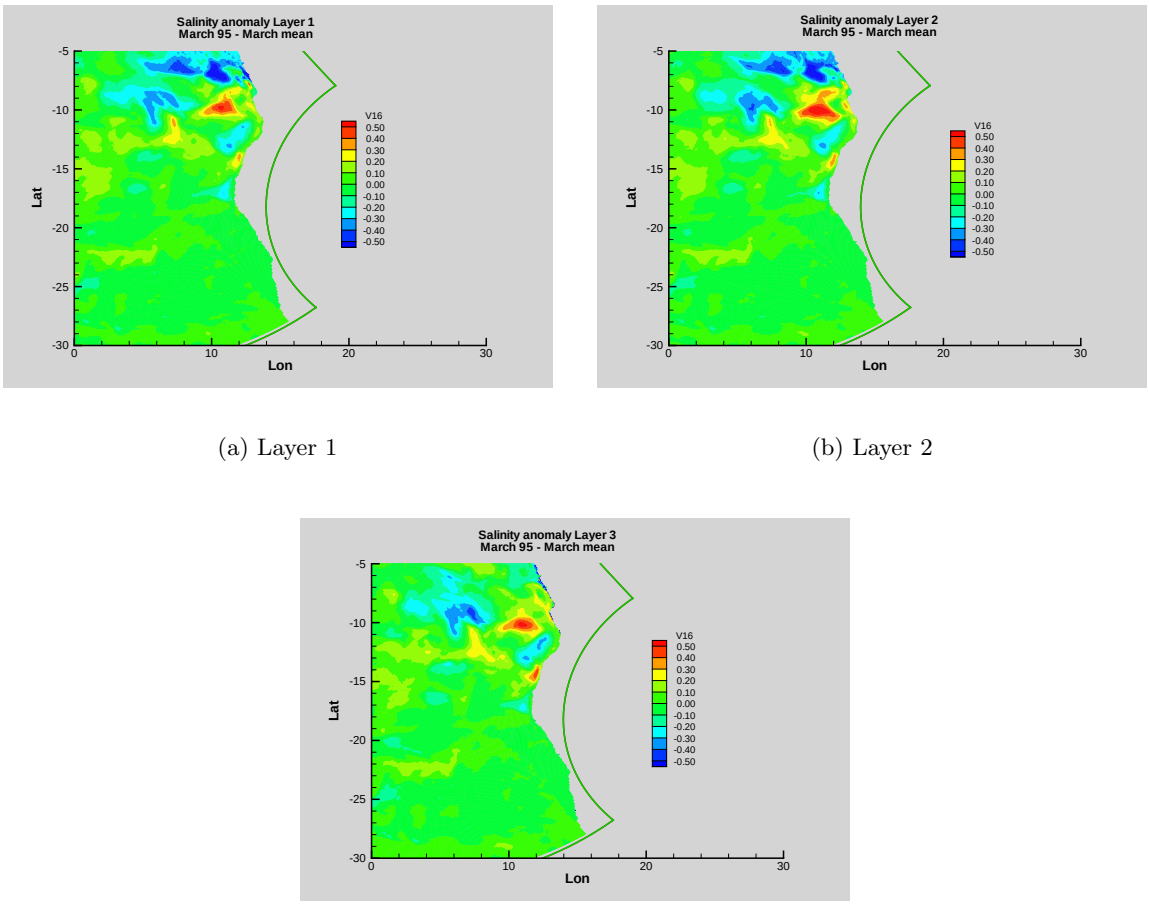

(a) Layer 1

(b) Layer 2

(c) Layer 3

Figure 4.7: *Salinity anomalies for March 95, layers 1, 2 and 3.*

close to the coast displays salinities below 34 psu. The salinity in the southern Benguela is relatively constant, with values between 35.2 and 35.4 psu through all the 4 layers. A tongue of low-salinity water is observed close to the coast at 14–18°S. It is more pronounced in the 3 upper layers; in layer 4 it is weaker but still visible. The overall picture of the salinity in March 95 resembles the average March conditions shown in figure 4.3.

A clearer view of any differences between the anomalous 1995 and the general trend is visualized by salinity anomalies as shown in figure 4.7. In layer 1 a negative anomaly with values up to 0.5 psu is observed in the far north, around 5–6°S. Around 10°S a positive anomaly of the same magnitude is seen. This anomaly is stronger in layer 2. The tongue of fresher water along the coast does not seem to be exclusive to 1995, as the anomaly plots do not show a consistent negative anomaly in this area. Both a weak positive and a weak negative anomaly of 0.2 to 0.3 psu are observed. Further south, in Namibian waters, the salinity in March 95 seems to be nearly identical to the general March conditions. The situation in the third layer resembles that of layers 1 and 2.

Sea Surface Height

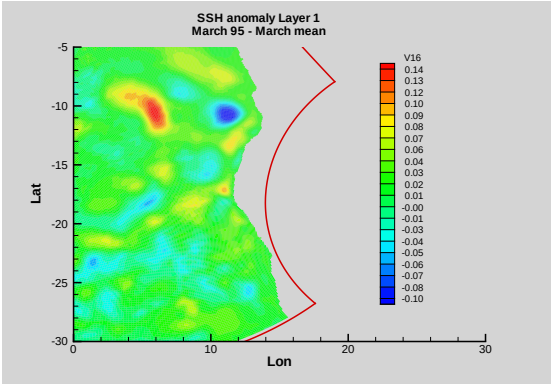

Figure 4.8: *The SSH anomaly at the surface in March 1995*

Figure 4.8 shows the sea surface height anomaly for March 1995. A positive anomaly extending over 2–3 degrees of latitude and 1 degree of latitude is seen in Angolan waters. Closer to shore, a negative anomaly of similar shape and size is present. Both have maximum values of around 10 cm. Further south there are patches of negative and positive SSH-anomalies, but no general trend is apparent.

4.2 Vertical sections

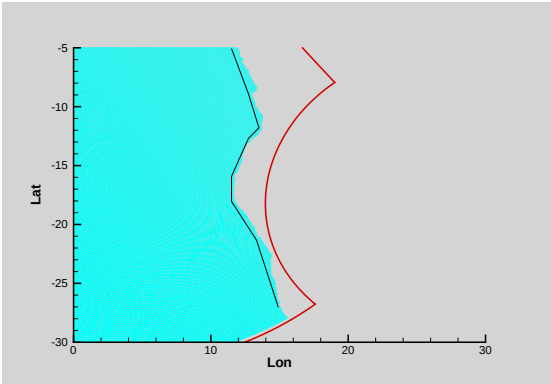

Figure 4.9: *The vertical section along the coast.*

The vertical sections available in Tecplot are taken along the gridlines, as shown in figure 3.1. This can make it difficult to look at specific areas of interest. A program developed by Knut Arild Lisæter at NERSC makes it possible to make vertical sections which follow the geodesic line (the curved geometry equivalent to a straight line in plane geometry) between two points on the earth. This routine, called m2t_geo, was used to create vertical section plots along the coastline of southwestern Africa. The position of this section is shown in figure 4.9.

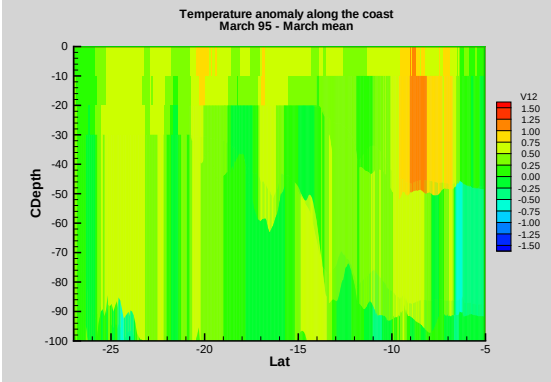

Figure 4.10: *The temperature anomaly in the upper 100 meters along the coast of Angola and Namibia in March 1995.*

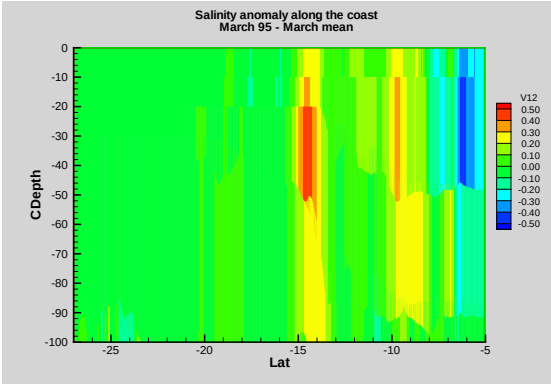

Figure 4.11: *The salinity anomaly in the upper 100 meters along the coast of Angola and Namibia in March 1995.*

Temperature

Figure 4.10 shows the temperature difference between March 1995 and the March mean along Africa's south-western coastline. The figure shows the upper 100 meters. The actual bottom depth of the section varies, but is generally between 100 and 500 meters. The results correspond to what was found in the horizontal sections. A positive temperature anomaly is seen at 7°S, and it extends to about 50 meters depth. This anomaly can also been seen close to the coast in figure 4.5. Further south, weak positive anomalies are found throughout the upper 100 meters, with magnitudes of up to 0.75°C.

Salinity

The salinity anomaly for the same section along the coast is shown in figure 4.11. The weak anomalies seen in the horizontal sections (figure 4.7) are evident. A positive anomaly of about 0.4 psu is located around 14°S at 20–50 meters depth. In the far north of the section a negative anomaly of 0.4 psu extends from 45 meters depth to the surface. South of 15°S, the salinity anomalies are insignificant.

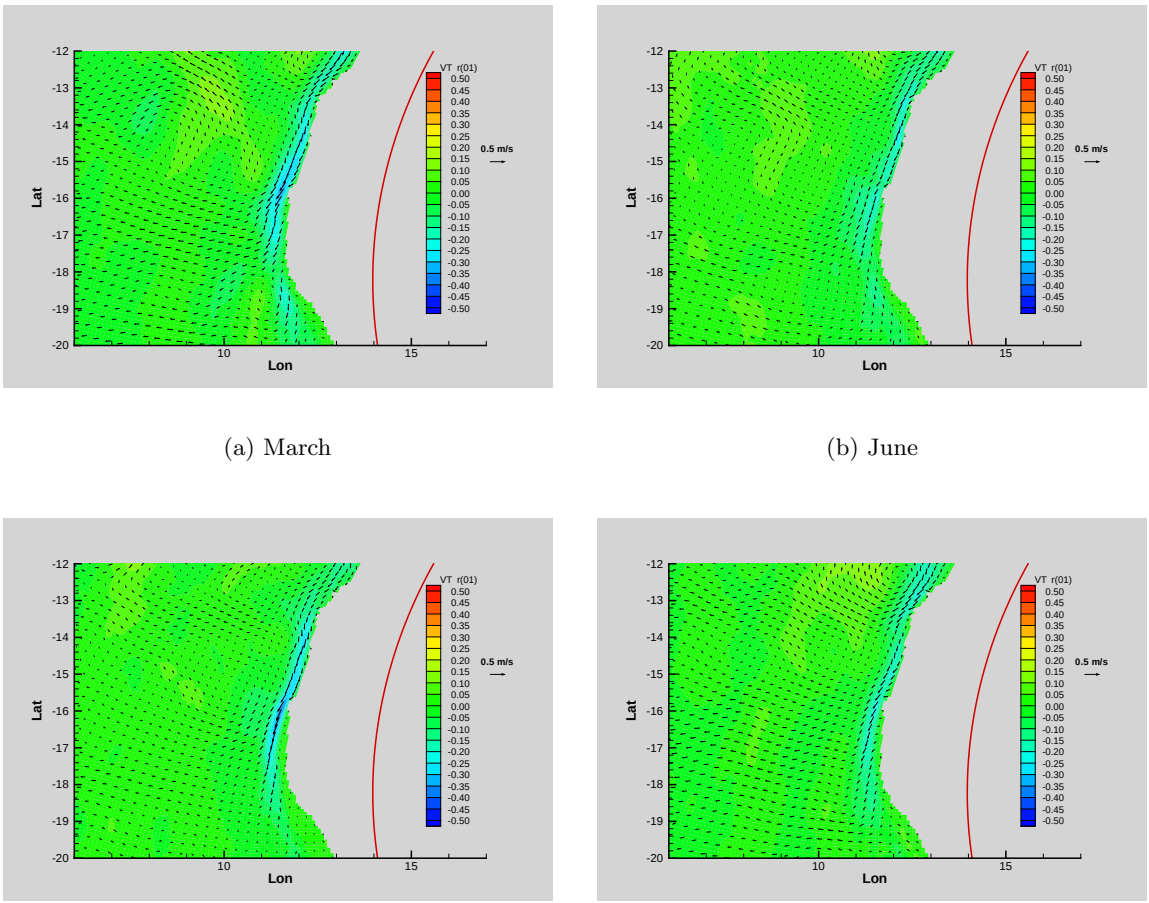

(a) March

(b) June

(c) September

(d) December

Figure 4.12: *Current vector-plots and north-south speed (color code) for the March, June, September and December mean*

4.3 Currents

In order to find out whether the model is able to describe the dynamics of the 1995 Benguela Niño, we look at the u- and v-velocities in horizontal and vertical sections.

4.3.1 Horizontal vector plots

As the Benguela Niño manifests itself as a unusually strong poleward intrusion of warm and saline water in the Angola-Benguela frontal zone, we look at the velocities in this area. Figure 4.12 shows the surface current patterns as well as the v-velocity (north-south, color code) for the monthly means of March, June, September and December. Most of the temporal and spatial variability has been averaged out, but the Angola Current along the coast between 12 and 18°S is visible in the model output.

The Angola current is according to the model data strongest in austral fall and spring

(March and September), with v-velocities up to 40 cm/s. In winter and summer (June and December) the poleward movement is weaker; the maximum v-velocity is approximately 30 cm/s. In all the seasons the current leaves the coast in a westward direction between 16°S and 18°S.

Figure 4.13 shows weekly averages from February and March 1995. The v-velocities are larger than in the monthly means, as short-term variability in time and space is less averaged out. Eddies and meanders are evident at 12–13°S and around 17°S throughout February and March.

In the first week of February shown in figure 4.13(a) the south-westward current along the coast has a maximum v-velocity of 40 cm/s in a limited area. There is poleward movement to about 19°S, but the flow is interrupted by eddies. The following week (figure 4.13(b)) shows a somewhat different picture; the current is moving faster in a southerly direction, and the velocities are close to 50 cm/s in a larger area. This trend continues in the third week (figure 4.13(c)). The current leaves the coast and travels in a westerly direction around 16.5°S, but there is an area of southward movement further south, between 18°S and 19°S. The v-velocities there are around 40 cm/s. The poleward current reaches a maximum in the last week of February (figure 4.13(d)), when v-velocities of up to 40 cm/s can be seen as far south as 19.5°S.

The situation in the first week of March (figure 4.13(f)) resembles the one during the previous week, but this changes when we get to week 2 in March. Then the velocities are much weaker, and the current is diverted away from the coast further north by the eddy seen at 17°S. There are still positive v-velocities in the far south of the section, but they are weaker than earlier. In the last week of March (figure 4.13(h)) the current seems to pick up the pace at 14–15°S, and a large eddy has developed close to this.

4.3.2 Vertical sections of velocity

A further investigation of the structure of the Angola Current during the 1995 Benguela Niño can be undertaken by looking at vertical sections of north-south currents along selected latitudes.

The vertical sections used here were taken across the Angola current at latitudes 15°S and 19°S. The northern section is from 11.5°E to 12.1°E, while the southern section is from 11.2°E to 12°E. The chosen time period is when the horizontal plots showed that the southward movement was at its strongest and then decreasing, from week 3 in February to the second week of March.

Sections along 15°S

The vertical structure of the section current in the upper 200 meters at 15°S is shown in figure 4.14. The surface signal seen in the horizontal plots extends to deeper layers. In the upper 50 meters the north-south velocity is high, with a maximum in the third week of February (figure 4.14(a)). During this week the velocities reach 80 cm/s in the three upper layers. Further down, around 50–100 meters depth, there is still movement towards the south,

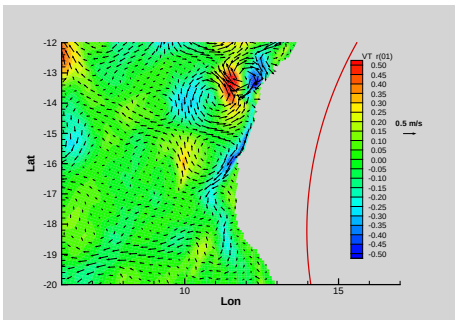

(a) Week 1 February

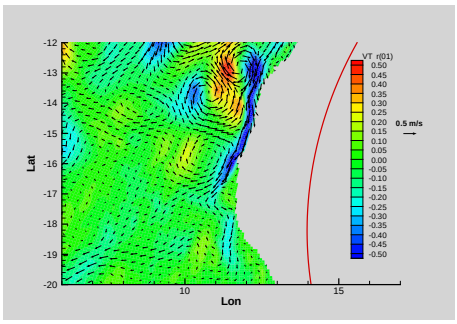

(b) Week 2 February

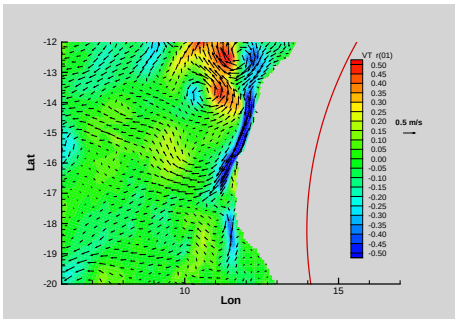

(c) Week 3 February

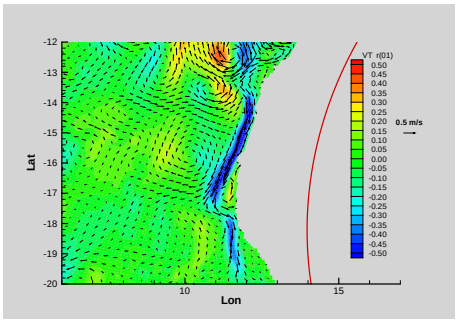

(d) Week 4 February

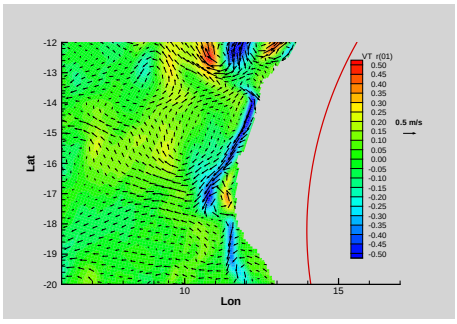

(e) Week 1 March

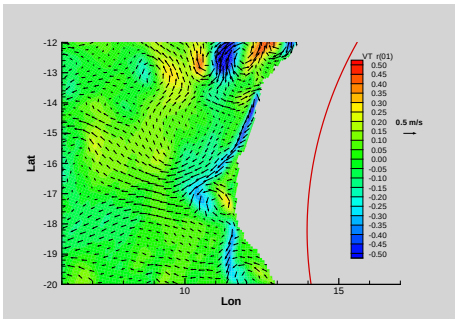

(f) Week 2 March

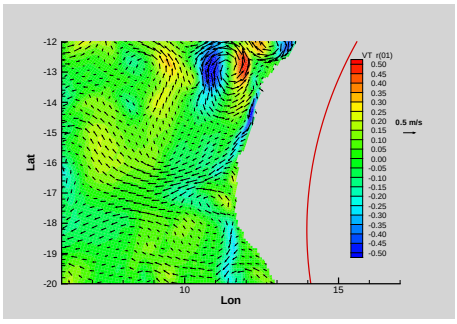

(g) Week 3 March

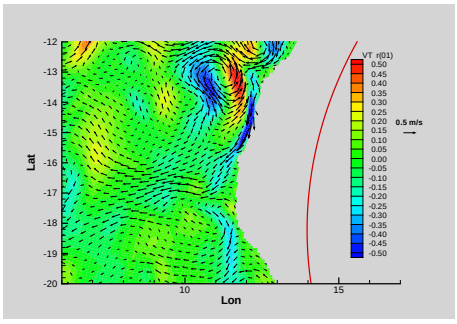

(h) Week 4 March

Figure 4.13: *Vector-plots and north-south velocity for weeks 1–4 in February and March 1995.*

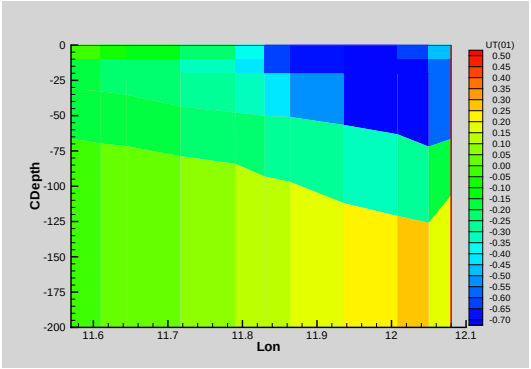

(a) Week 3 February

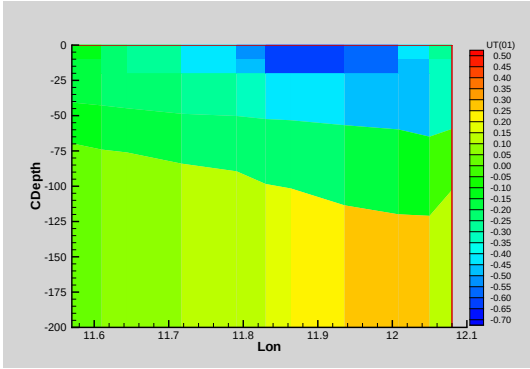

(b) Week 4 February

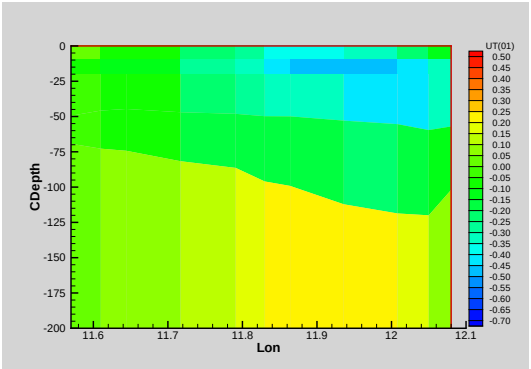

(c) Week 1 March

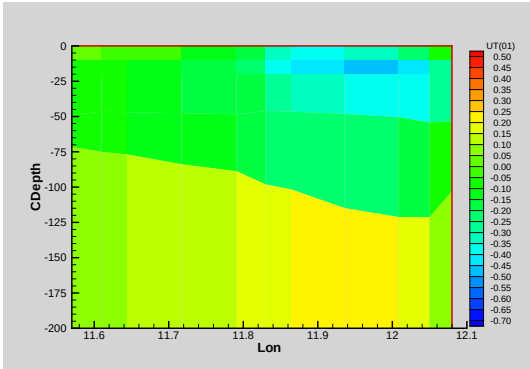

(d) Week 2 March

Figure 4.14: *Velocity across the section 15°S 11.5–12.1°E for week 3 and 4 in February 1995 and week 1 and 2 in March 1995.*

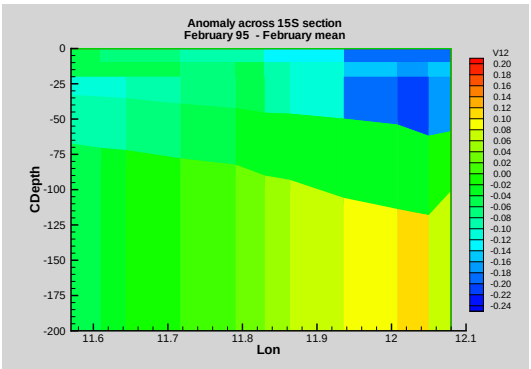

(a) February

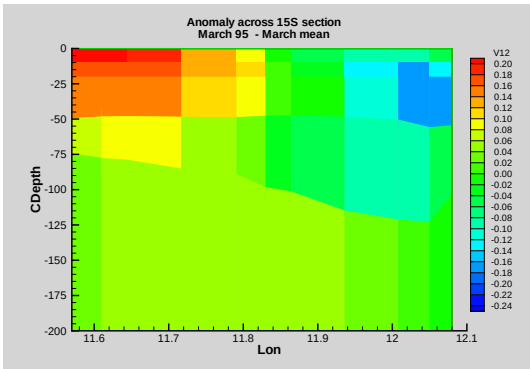

(b) March

Figure 4.15: *Anomaly of velocity across the section at 15°S, 11.5–12.1°E.*

but the velocities are lower, around 30 cm/s. Below 100 meters depth, the water close to the coast is moving northwards.

The vertical sections show that the poleward velocities are highest in the end of February and decreasing during the two first weeks of March. The maximum velocities throughout the time period are found in layer 2, which is located between 10 and 20 meters depth.

Figure 4.15 shows the anomalies of north-south velocity for February and March 1995. The southward velocity in February 1995 is stronger than for the February mean; near the coast (around 12°E) the negative anomalous values reach 25 cm/s. The anomaly plot for March shows a similar picture for the coastal areas, with somewhat smaller values (up to 18 cm/s). A positive anomaly is seen in the western part of the section, with northward velocities of up to 20 cm/s.

Sections along 19°S

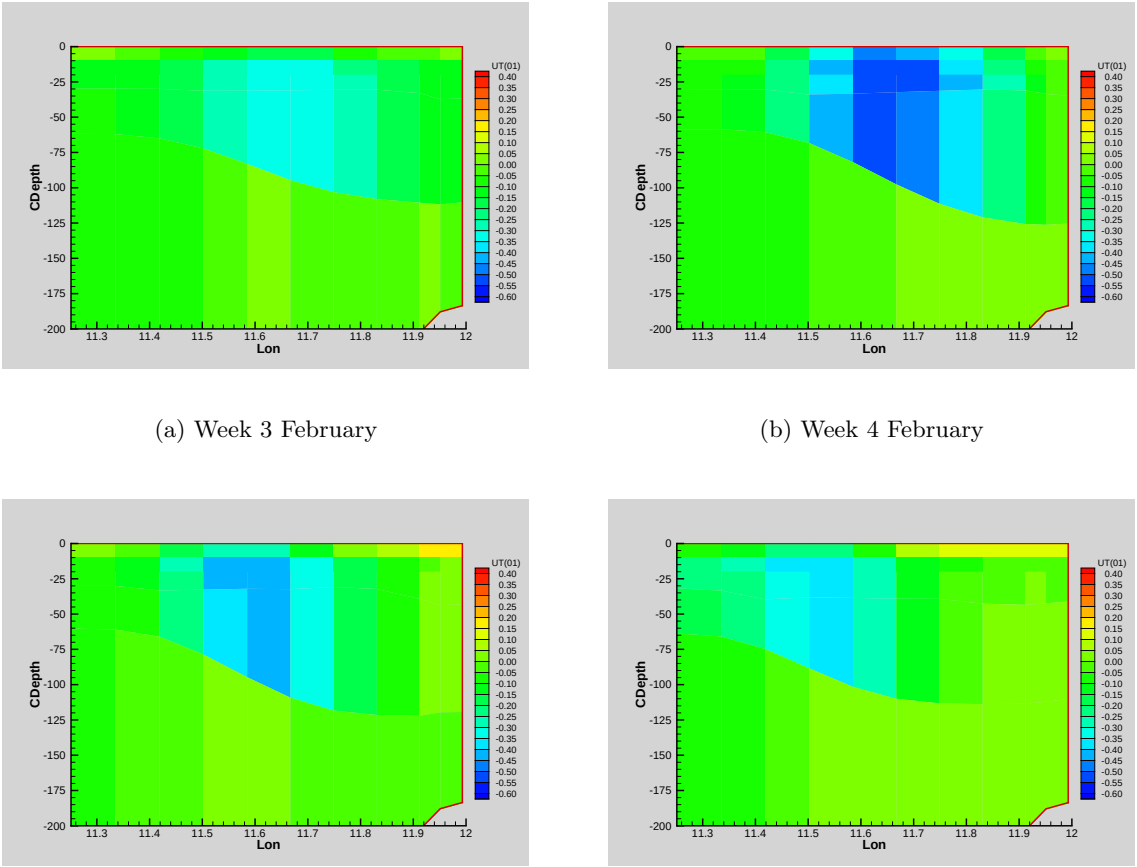

(a) Week 3 February

(b) Week 4 February

(c) Week 1 March

(d) Week 2 March

Figure 4.16: *Velocity across the section 19° S 11.2–12° E for week 3 and 4 in February 1995 and week 1 and 2 in March 1995.*

Figure 4.16 shows the vertical sections taken along 19°S. This section covers the south-

ernmost part of the Angola Current, as seen in the horizontal plots in figure 4.13. Both the vector plots and streamtrace plots (a function in Tecplot which can show the origin of currents) show that the water in this southern branch originates from the main part of the Angola Current. Note that a different velocity scale is used. In week 3 in February (figure 4.16(b)), the most pronounced southward movement is seen between 11.5°E and 11.8°E in layers 2–4. The velocities range between 25 and 35 cm/s. The highest southward velocities are observed in the last week of February, with values up to 60 cm/s at depths between 10 and 75 meters. The first two weeks of March show a similar structure, but with lower values. The area of poleward velocities also seems to been moving slightly westward during this time period.

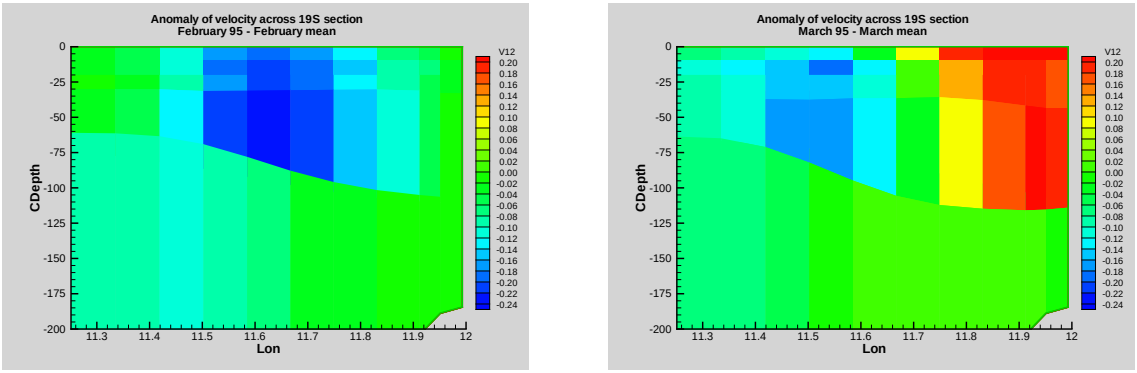

(a) February (b) March

Figure 4.17: *Anomaly of velocity across the section at 19° S, 11.2–12° E.*

The velocity anomalies across the section for February and March are shown in figure 4.17. In February 1995 the southward movement reaches a magnitude of 25 cm/s when compared to the monthly mean for the same month. In the following month a negative anomaly is observed a bit further west, with values of approximately 18 cm/s. Closer to shore a positive anomaly is observed; in March 1995 the water around 12°E moves in a northward direction with velocities of more than 20 cm/s.

Chapter 5

Discussion

5.1 Comparison of model data and observations

5.1.1 Horizontal sections

In the previous chapter, a number of horizontal plots of the model output were presented. The main focus was on March 1995, which is when the previous Benguela Niño took place. We will now do a composite analysis of the model data and available observations to see how the model performs.

Monthly means

The general structure of the temperature and salinity distribution in the 15-year monthly means presented in chapter 4 is consistent with the in situ records from the area. However, the absolute values of the temperatures and salinities seem to differ somewhat from the observations. For instance, a comparison with mean monthly SST in the northern Benguela (Cole & Villacastin 2000) reveals that the temperatures in the upwelling area are lower in the observations than the model data. Cole & Villacastin (2000) found temperatures as low as 11°C in the coastal Benguela area, while the corresponding values from the model plots are around 17°C. In the north, the model temperatures appear to be too low compared with observational data. The model seems to have difficulties with temperature gradients in the horizontal fields.

1995 Temperature

The horizontal plots of temperature in the 4 upper layers shown in figure 4.4 are not consistent with the observed temperatures from the same time period. A comparison of layer 1 with ship measurements of SST from March 95 (Gammelsrød et al. 1998) shown in figure 5.1 reveals that the model temperatures are generally too low in the north and too high in the upwelling areas in the south. The isoline for 29°C in the observed data is seen as far south as 15.5°S. In the model data, water of this temperature is only detected in the far north, reaching 7°S at its maximum poleward extension. The plot of the surface layer gives the mean values for the upper ten meters, and this could result in a somewhat lower surface temperature in the

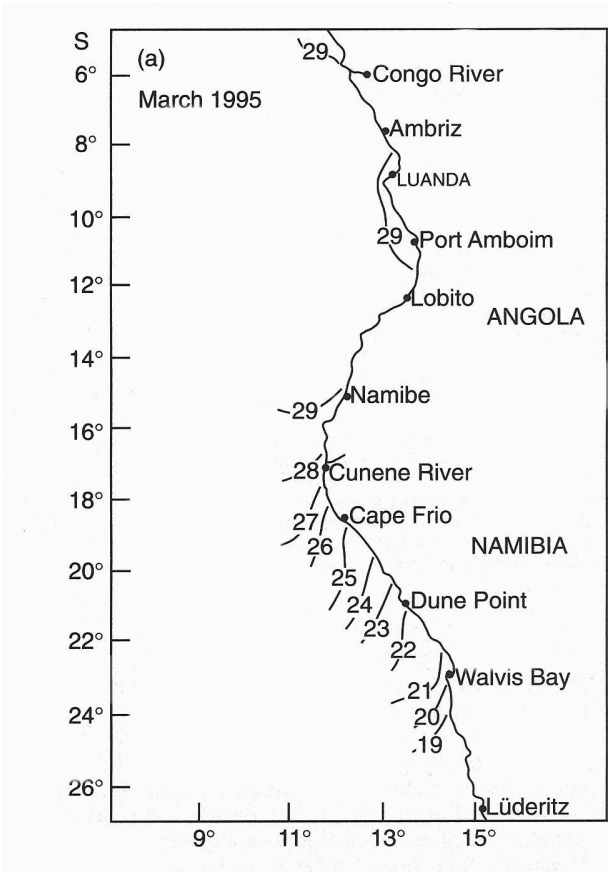

Figure 5.1: *Sea surface temperature distribution from ship measurements in March 95. From Gammelsrød et al. (1998).*

model data. However, the difference between the model temperatures in the upper layer and the observed SST is still striking.

The plots of the deeper layers (2–4) show no signs of a warm intrusion from the north. The temperature is as expected decreasing with depth.

The deviation between the model temperatures and the observations becomes even more evident when we look at the anomalies. Figure 5.2 shows the differences in the horizontal distribution of temperature at 30 meters depth off Angola and Namibia. Gammelsrød et al. (1998) found that the intrusion of warm water had a maximum temperature difference at 20–40 meters depth, and it is therefore appropriate to look at layer 3 when comparing the model data with in situ observations. A comparison with the model temperature anomalies, shown in figure 4.5, reveals that the model does not seem to describe the anomalous temperature conditions during the 1995 Benguela Niño very well. Both the structure and the maximum value of the positive temperature anomaly in the model differ from the observational data. The maximum observed temperature difference was 8°C, off Cape Frio (18°S). The corresponding anomaly in the model data in the same area is in fact negative. It seems like the numerical model WANE struggles to provide an accurate description of the sea temperature, especially during anomalous conditions. Possible reasons for that will be discussed later.

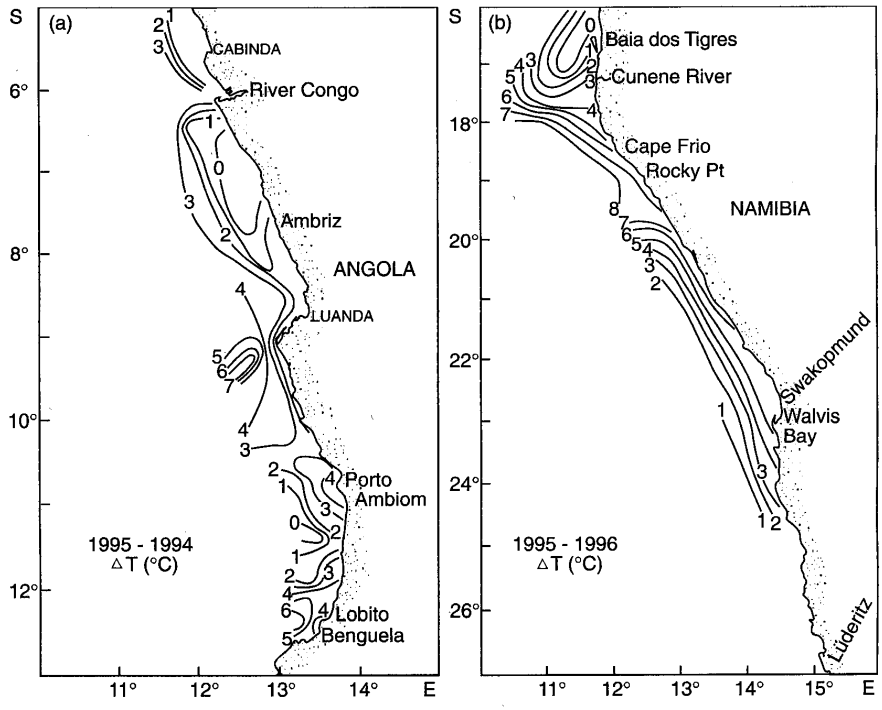

Figure 5.2: *Differences in the horizontal distribution of temperature in March at 30 meters depth off a)Angola 1995–1994 and b)Namibia, 1995–1996. From Gammelsrød et al. (1998).*

1995 Salinity

Figure 5.3 shows the salinity difference between 95–94 and 95–96 off the coast of Angola and Namibia (Gammelsrød et al. 1998). When comparing this with the monthly mean salinity anomaly for the corresponding area in the model (figure 4.3), it is clear that the correspondence between the two is rather poor. The salinity anomalies shown in figure 5.3 are at 4 meters depth, so although the differences between the model anomalies in layers 1 and 2 are not very significant, the emphasis is put on the former.

The observed negative anomaly in the north and the weaker positive anomaly in southern waters described in chapter 2 is not seen in the model data. This also becomes evident when looking at the salinity in the 4 top layers (figure 4.6). The fresh surface water observed around 18°S in March 1995 (Gammelsrød et al. 1998) is not seen in the model data. The monthly model anomalies do reveal weak anomalies of up to 0.5 psu, but they are too weak and located too far north. The model is apparently not able to describe neither the temperature nor the salinity variations observed during the 1995 Benguela Niño.

1995 Sea Surface Height

The observed positive sea surface height anomaly of up to 20 cm during the 1995 Benguela Niño shown in figure 2.6 is not detected in the model data (figure 4.8).

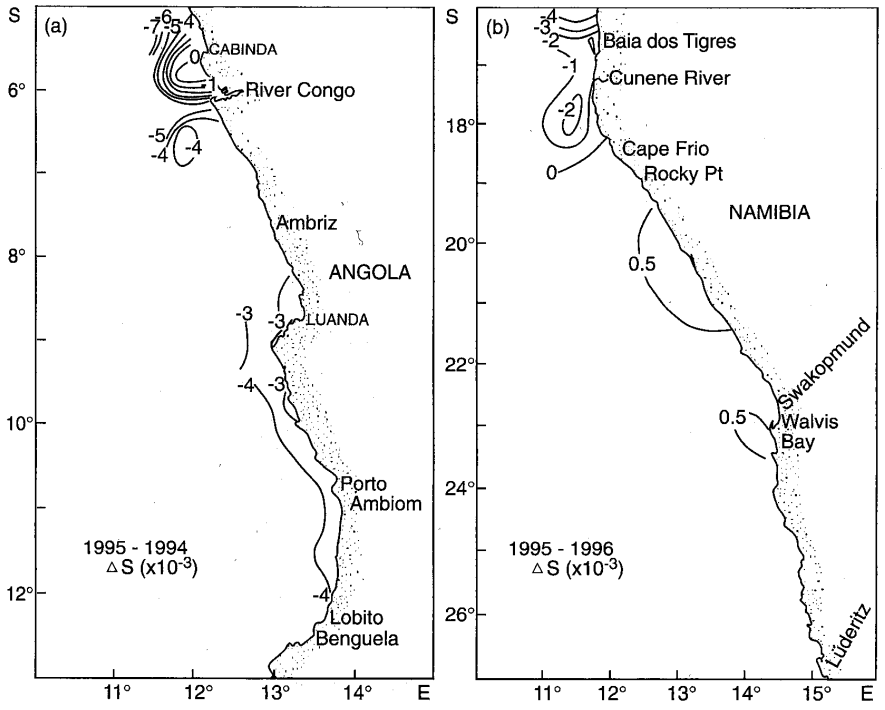

Figure 5.3: *Differences in the horizontal distribution of salinity at 4 meters depth in March off a)Angola 1995–1994 and b)Namibia, 1995–1996. From Gammelsrød et al. (1998).*

5.1.2 Vertical sections

1995 Temperature

The lack of accordance between the observations and the model data can also be illustrated by looking at a vertical section along the coast. Figure 5.4 shows the temperature and salinity anomalies in a section parallel to the coast near the 100 meters isobath. The vertical section for the same area from the model is seen in figure 4.10. The positive temperature anomaly at about 20 meters depth around 20°S is not visible in the model data. The maximum temperature difference observed in the model results has a magnitude of just over 1°C, while the corresponding value for the measurements is 7°C. The data used to compute the anomaly in the model data is the March mean, while observations from March 1996 was used to calculate the observed anomaly, and this could explain some of the differences. The poor accordance between the observations and the model data still indicate the model's problems with reproducing temperature.

1995 Salinity

The lower part of figure 5.4 shows the vertical section of the salinity anomaly derived from observational data. A comparison with the model vertical section shown in figure 4.11 reveals another example of the model's poor description of extreme temperature and salinity conditions. Neither the negative salinity anomaly in the surface around 13–14°S nor the

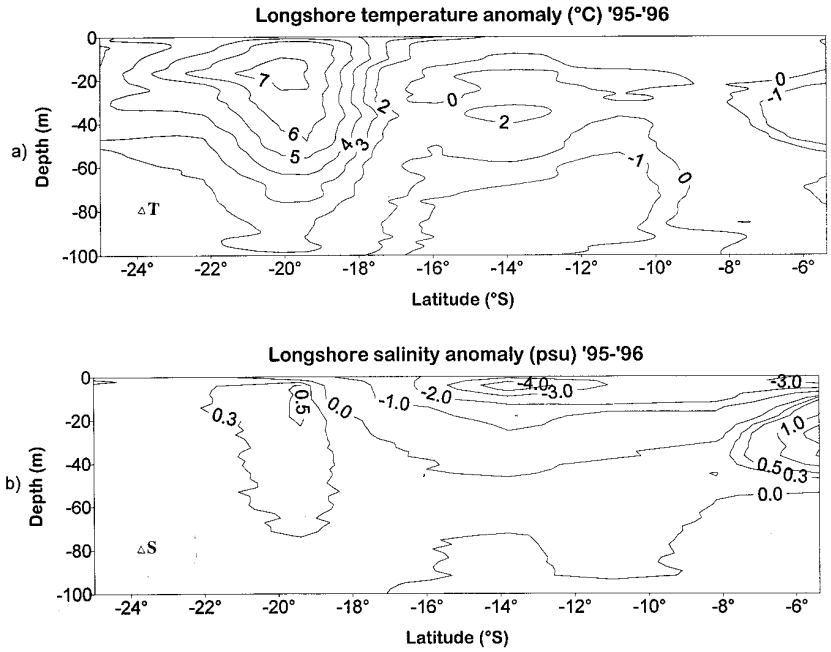

Figure 5.4: *Differences in the vertical distribution of a) temperature (ΔT) and b) salinity (ΔS) between March 1995 and March 1996 in a section parallel to the coast near the 100-m isobath. From Gammelsrød et al. 1998.*

weaker positive anomaly seen at approximately 10–20 meters depth around 19–20°S in the observations are apparent in the model data. Accordingly, the positive and negative salinity anomalies in the model data do not have any similar counterparts in the observational data.

5.1.3 Currents

Horizontal vector plots

The horizontal vector plots shown in figure 4.13 show a higher correlation with the observations. The maximum poleward velocities in the model data are seen during the last weeks of February, just before the strongest signal of the 1995 Benguela Niño was observed. Gammelsrød et al. (1998) found that the maximum southward extent of the anomaly was observed during the first week of March 1995, and the velocity plots from the model show that the southward current weakens from week 2 in March 1995.

In order to examine the ocean currents in the Benguela during the 1995 Benguela Niño, we look closer at the drifter shown in chapter 2. In figure 5.5 the drifter path is plotted next to February 95 from the model. The color code shows the north-south velocity (positive towards the north), and the current is plotted by vectors. We can see that the drifter's initial movement corresponds to the predominant current structure; the current in the model is mainly northwestward in the area the drifter was released, and the buoy moved in the same direction during the first week of its deployment.

Figure 5.6 shows the currents according to the model in more detail. The weekly means

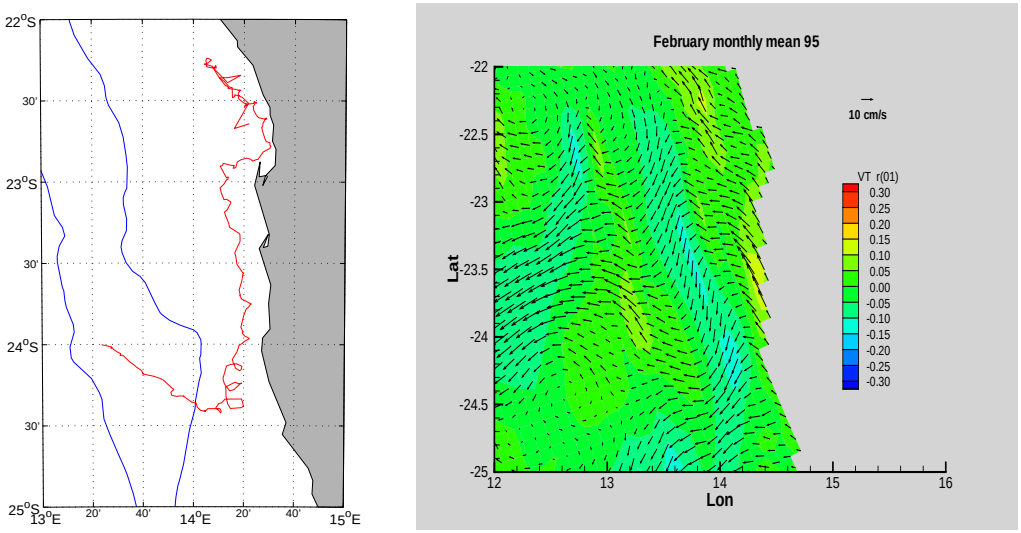

(a) (b)

Figure 5.5: *The drift path of the surface drogue described in chapter 2 (a) and current vector-plots and north-south speed (color code) for February 95 from the model (b).*

from the second week of February to the first week of March reveal that the north-westward current dominating in the area in question during the first two weeks has the same direction as the drifter's initial movement. During the last week of February, the current seems to weaken and shift to a more southerly direction. This coincides with the drifter's strongest southward movement. Although the speed seen in the plots from the model is not as high as the observed velocity, this could be another indication that the model is able to describe the dynamics of the Benguela Niño better than it simulated the temperature and salinity.

Vertical sections of velocity

The vertical sections confirms the picture of the surface currents shown in the previous section, and also shows us the vertical structure of the Angola Current.

As seen in figure 4.14 and figure 4.16, the northern section has a maximum southward velocity during the third week of February(15°S, 12°E), while the maximum further south is seen one week later (19°S, 11.6°E). After that the southwards currents weaken. This indicates that the poleward current is stronger during February-March 1995, and this concurs with the observations of the 1995 Benguela Niño. As seen in the horizontal plots, the southward current weakens after the peak of the anomaly.

The anomaly plots in figure 4.15 and figure 4.17 shows that the velocity in February and March 1995 were indeed larger than normal, with values up to 25 cm/s. This corresponds with other model results, where anomalous currents of 20 cm/s were seen in February 1984 (Carton & Huang 1994).

When looking at the Angola current, it seems like WANE is more successful at simulating

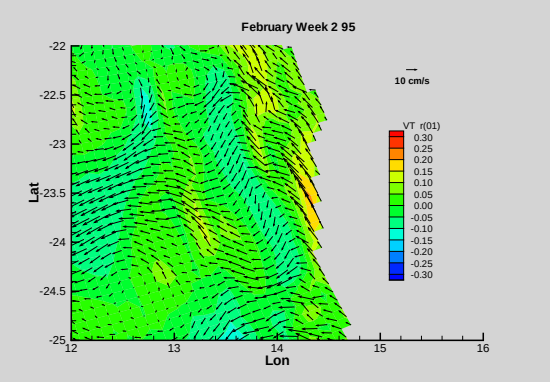

(a) Week 2 February

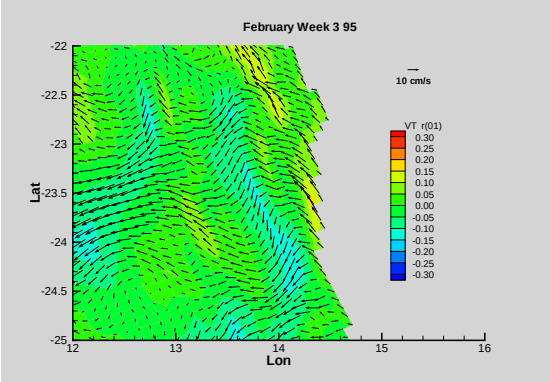

(b) Week 3 February

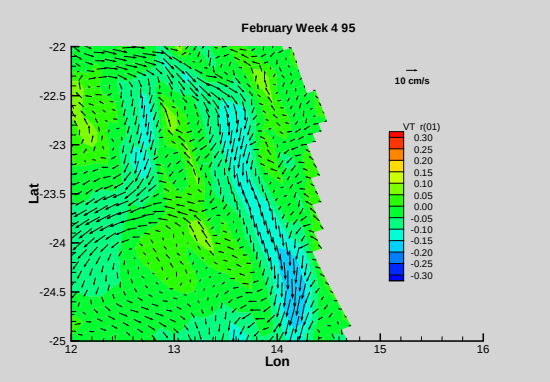

(c) Week 4 February

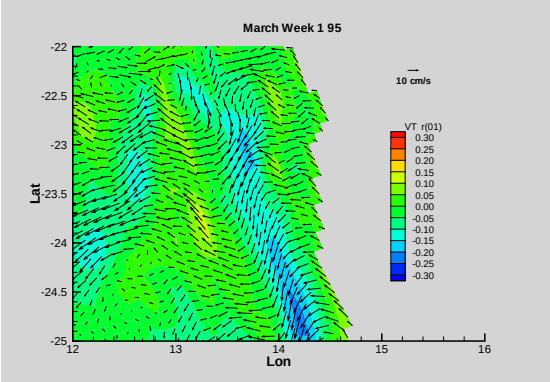

(d) Week 1 March

Figure 5.6: *Current vector-plots and north-south speed (color code) for week 2 (a), 3 (b) and 4 (c) in February and week 1 in March (d).*

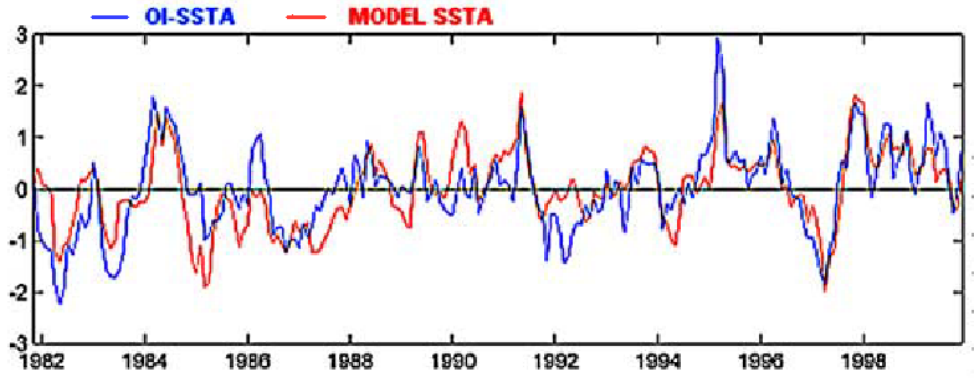

Figure 5.7: *OPA SST and OI-SST anomalies from 1982 to 1999, averaged over 10–20°S and from 8°E to the coast. From Florenchie et al. (2003).*

this current during the 1995 Benguela Niño. These results are in agreement with previous studies of the WANE model; it was able to produce good results for oceanic currents (Evensen et al. 2002). The model's inability to adequately describe the temperature and salinity conditions is still a major concern, so we will now look at how other models have performed in this respect.

5.2 OPA version 8 Ocean General Circulation Model

Other numerical ocean models have had more success at describing the thermohaline signal of the 1995 Benguela Niño. The ocean general circulation model OPA (Ocan Paralllis) was developed at the Laboratoire d'Ocanographie Dynamique et de Climatologie (LODYC) in Paris, France. Florenchie et al. (2003) used output from this model as well as Optimal Interpolated Sea Surface Temperatures (OI-SST) to study the warm event in the Benguela in 1995.

5.2.1 OPA results

Florenchie et al. (2003) compared the OI-SST satellite data set described in (Reynolds & Smith 1994) with the OPA SST, and the results are shown in figure 5.7. It shows the history of the SST anomalies averaged from 10–20°S and from 8°E to the coast from 1982 to 1999. The figure shows a good correlation between the model data and the OI-SST, and the surface signals of the documented warm events in 1984 and 1995 are both visible. According to Florenchie et al. (2003) the sea surface height anomalies from the model are in good accordance with observations from satellite altimetry, and this indicates that the model also gives a satisfactory description of the subsurface conditions.

A vertical section of the model's SST anomalies along the coast from March 1984 is shown in figure 5.8. This figure is from 1984, but the model displayed similar results for the 1995 event (Florenchie et al. 2003). A comparison between the observations in figure 5.4 reveals that the structure of the temperature anomaly below the surface in the OPA model resembles

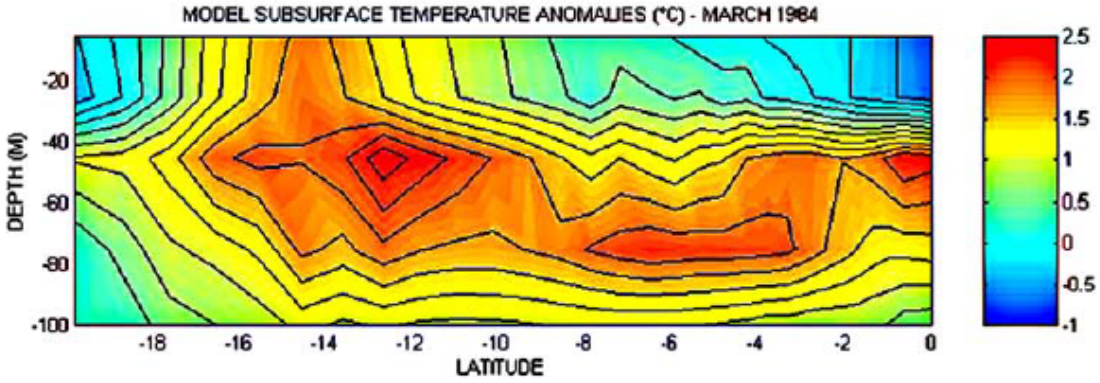

Figure 5.8: *Vertical section of the monthly mean temperature anomalies along the coast in March 1984. From Florenchie et al. (2003).*

the observations, although the maximum signal of the anomaly is weaker and it is located further north. The structures of the vertical sections are similar, and it is clear that OPA is able to recreate the subsurface signal of the Benguela Niño.

In conclusion, the OPA ocean general circulation model seems to be better at describing the temperature and salinity conditions of extreme events in the southern Atlantic than WANE. The possible reasons for the different model results are explored in the next section.

5.2.2 Differences between OPA and WANE

OPA is a primitive equation model which can be applied to both regional and global ocean circulation. It uses the Boussinesq, rigid lid and hydrostatic approximations (Madec et al. 1998). From 1979 to 1991, the OPA model is forced by wind stress fields from the European Center for Medium-Range Weather Forecast (ECMWF) reanalysis, while satellite ERS wind stresses are used for the remainder of the integration period (1992–1999) (Florenchie et al. 2003).

Although there are differences between OPA and WANE in terms of i.e. the choice of vertical coordinates (OPA uses z- and sigma-coordinates), the main reason for the discrepancies between the two models is probably found in the use of climatology and background data. OPA used the Levitus climatology for initialization of the model, while the variables that forced the model (daily wind stress, net surface solar radiation, net surface heat and freshwater fluxes) were taken from various sources, including re-analyses and observations. WANE was initialized by using interpolation from a larger scale model (WAX). The wind data were based on the NCEP re-analysis, and the surface fluxes of heat and freshwater were relaxed towards the Levitus climatology.

Under the same conditions, with equal setup and forcing, the two models should produce similar results. However, there are some major differences between OPA and WANE. Firstly, the surface fluxes in WANE are relaxed towards climatology, and this dampens any large variations and keeps anomalous conditions from developing. The OPA surface temperature is relaxed towards observations (Florenchie et al. 2003), and this enhances SST-anomalies.

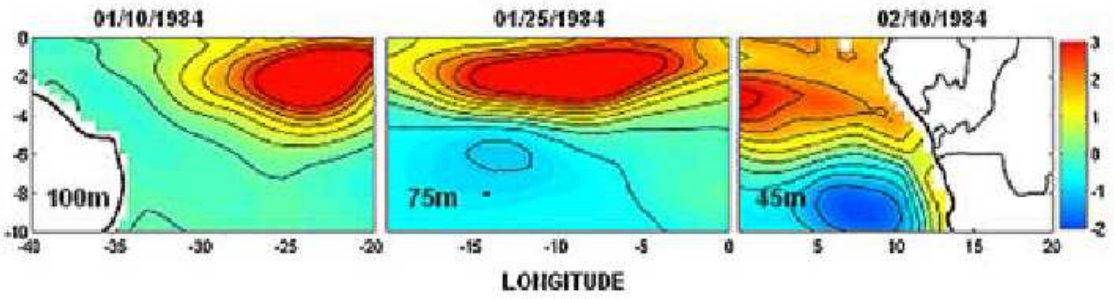

Figure 5.9: *The movement of the temperature anomaly across the Atlantic during the first two months of 1984. First panel: 10.01.84, 100 m. Second panel: 25.01.84, 75 m. Third panel: 10.02.84, 45 m. From Florenchie et al. (2003).*

If the Benguela Niño is triggered by atmospheric forcing (heat), this will be sufficient to generate it in OPA while WANE will have no chance of developing it. The OPA model is also able to reproduce the subsurface signal of the warm event, which is coupled to the surface signal. Without the surface signal there would be no subsurface signal.

Another possible factor could be the wind-stress data used in the models. While the wind-stress fields used in WANE were taken entirely from the Oceanweather Inc. adaptation of NCEP data, OPA used a combination of re-analyses and observational data. The wind-stresses in WANE are accurate compared to ECMWF-data, but observed wind data may be even better. In the following section we will explore how the wind and the Benguela Niños are related.

5.3 Forcing mechanisms for Benguela Niños

As seen in chapter 2, the Benguela Niño is believed to be triggered by variations in remote wind patterns, more specifically a relaxation of the trade winds off the coast of Brazil. This is supported by numerical simulations.

The OPA model did not only display the temperature anomalies observed during a Benguela Niño, it was also able to show the preceding Kelvin wave moving across the equatorial Atlantic. This is shown in figure 5.9. Florenchie et al. (2003) followed the 1984 anomaly back to its source and found that the maximum temperature anomaly could be detected at 30°W just south of the equator in the beginning of January. One month later, the anomaly had crossed the Atlantic and was about to start its poleward movement. The anomaly's eastward propagation was about 1.7 m/s, which is consistent with the theoretical phase speed of an internal Kelvin wave. The anomaly started out at the bottom of the mixed layer, and by the time it reached the African coast it was located at about 45 meters depth. The core of the anomaly followed the thermocline closely; it was located close to the 23°C isotherm. The displacement of the thermocline in the western equatorial Atlantic could be the result of sudden modifications of the trade wind in the same area. Florenchie et al. (2003) found that both the 84 and 95 Benguela Niño were preceded by changes in the average wind stress of between 25 to 50 %.

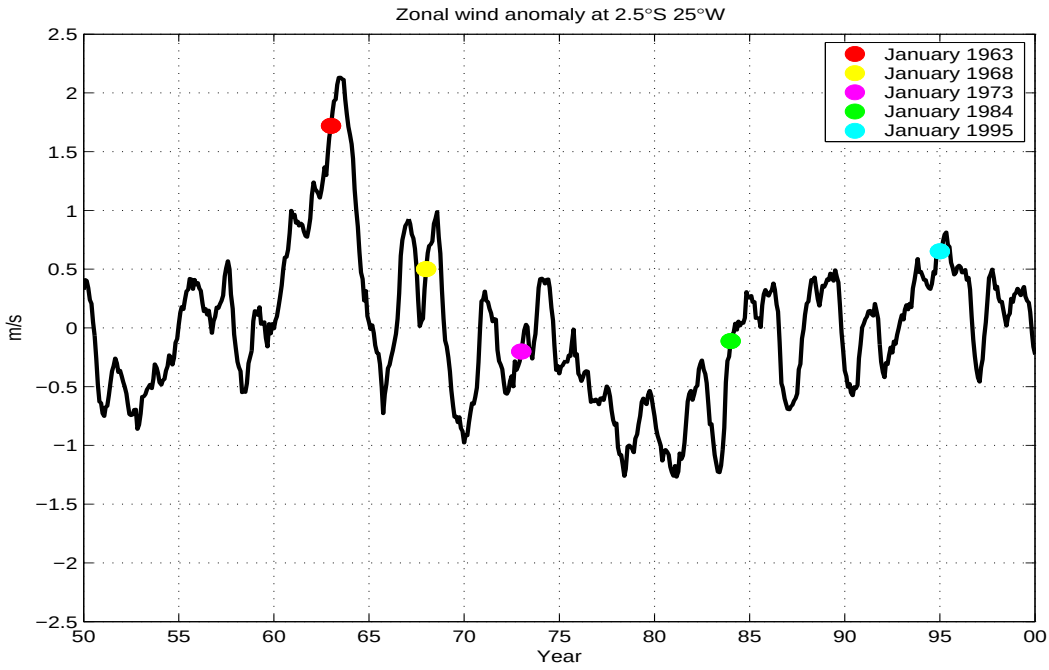

Figure 5.10: *Zonal wind anomaly at 2.5° S 25° W. Monthly means from 1950 to 2000. Wind data from NCEP*

A similar conclusion was reached by Carton & Huang (1994). By studying numerical model simulations and wind stress, they found that the main cause of the warming during the 1984 Benguela Niño was anomalous wind fields in the western basin. The presence of unusually warm water in the western Atlantic combined with a relaxation of the stronger than normal trade winds off Brazil in late 1983 led to a surge of heat into the Gulf of Guinea, which then continued poleward along the south-western coast of Africa (Carton & Huang 1994).

A time series of the zonal wind anomaly in the western equatorial Atlantic is shown in figure 5.10. The anomaly of the east-west component of the wind at 2.5°S 25°W was calculated by using monthly wind data from NCEP. This is close to where both Florenchie et al. (2003) and Carton & Huang (1994) found the largest changes in zonal wind. The markers show January of the years of the last three major Benguela Niños: 1963, 1984 and 1995, as well as two years (1968 and 1973) with warm events in the Benguela.

The zonal wind anomaly is by far largest in 1963, with values above 2 m/s. The years leading up to this maximum show a steady decrease in the easterly winds. The fact that the maximum anomaly through the 50 year-long time series coincides with a Benguela Niño suggests a relationship between the winds of Brazil and warm events in the Benguela. There have been indications of warm events in the Benguela in 1968 and 1973 (Binet et al. 2001). These years also display local maxima in the zonal wind anomaly, as seen in figure 5.10.

Figure 2.4 in chapter 2 shows the zonal wind anomaly in addition to the sea level anomaly for the 1984 Benguela Niño. The wind anomaly follows the sea level anomaly closely; there is a persistent negative anomaly through 1982 and 1983, which is followed by a sudden relaxation of the zonal wind between November 1983 and January 1984. To a certain degree, the NCEP

data for the same time period correspond with these results. Although the anomaly is not as strong as in 1963, there is a rapid change in the zonal wind during the months before the 1984 Benguela Niño, from August 1983 to January 1984. The 1995 Benguela Niño is also characterized by a local maximum in the zonal wind anomaly. The change is not as sudden as for the previous warm events, but the positive anomaly is the largest since the 1960s.

In conclusion, all the Benguela Niño years are characterized by a local maximum in the zonal wind anomaly during austral spring, with the highest value in 1963. The maximum positive anomalies generally coincide with the strongest thermohaline signal of the Benguela Niño on the other side of the Atlantic, off Angola and Namibia. Preceding the warm event, there is a change in the zonal winds for all the Benguela Niño years, but it is difficult to draw a final conclusion about how the winds off Brazil are connected to the generation of Benguela Niños from figure 5.10.

Chapter 6

Summary and conclusion

A comparative analysis of model data from the numerical ocean model WANE and available observations revealed that the model was unable to detect the thermohaline signals of the 1995 Benguela Niño. The model results did not show the temperature and salinity anomalies observed during the warm event, and the main reason for this is probably the relaxation of the surface fluxes towards climatology.

Although the outer model (WAX) which was used for initialization of WANE covers the entire South Atlantic and hence would be able to detect a Kelvin wave moving across the equatorial Atlantic, the WANE model seemed unable to reproduce that chain of events. Due to the open boundaries, a Kelvin wave generated in the WAX model in the south-western Atlantic should propagate into the WANE model. However, an even stronger relaxation towards the surface fluxes was used for the WAX model, so it probably experiences the same problems as WANE with respect to simulations of the Benguela Niño.

The WANE model is more successful at describing the current systems. This has previously been shown for the greater current systems in the area, and that was to a certain degree confirmed when looking for the Benguela Niño. The WAX and WANE models were primarily developed for a statistical simulation of the general current system along the west African coast, and not for studying the Benguela Niño. Surface relaxation was used as a precaution to ensure that there would be no unphysical drift in the model, risking poor representation of the water masses.

An investigation of the movements of a drifter buoy and winds during the 1995 Benguela Niño revealed a strong poleward current that moved against the southerly winds, indicating that local winds are not the main driving force of the phenomenon. The east-west component of the wind in the western equatorial Atlantic was examined, and there seems to be a relationship between the winds of Brazil and the Benguela Niños. Both numerical model simulations and the wind data support the governing theory of the generation and forcing mechanisms of Benguela Niños.

Further work could include a study of the general conditions in the model WANE to examine whether the temperature and salinity are in better accordance with observations when there is no warm event. A further investigation of the Benguela Niño could be conducted by running the model without surface flux relaxation, or even with assimilated surface SST

observations.

It is advisable to study the Benguela Niño further using both numerical models and observational data. The next Benguela Niño is expected in 2006, and due to the severe impacts on the biota and the local fishery industry, it is advisable to use more suitable models as well as collecting measurements from the area to increase our knowledge about this phenomenon.

Bibliography

Bearman, G., Brown, J., Colling, A., Park, D., Philips, J., Rothery, D. & Wright, J. (1998), *Ocean Circualtion*, Open University, Butterworth-Heinemann.

Binet, D., Gobert, B. & Maloueki, L. (2001), 'El Niño-like warm events in the Eastern Atlantic (6°N, 20°S) and fish availability from Congo to Angola(1964–1999)', *Aquat. Living Resour.* **14**, 99–113.

Bleck, R. (2002), 'An oceanic general circulation model framed in hybrid isopycnic-Cartesian coordinates', *Ocean Modelling* **4**, 55–88.

Boyd, A., Salat, J. & Maso, M. (1987), 'The seasonal intrusion of relatively saline water in the shelf off northern and central Namibia', *South African Journal of Marine Science* **5**, 107–120.

Carton, J. & Huang, B. (1994), 'Warm Events in the Tropical Atlantic', *Journal of physical oceanography* **24**, 888–903.

Cole, J. & Villacastin, C. (2000), 'Sea surface temperature variability in the northern Benguela upwelling system, and implications for fisheries research', *International Journal of Remote Sensing* **21**, 1597–1617.

Dümenil, L., Isele, K., Liebscher, H., Schröder, U., Schumacher, M. & Wilke, K. (1993), 'Discharge data from 50 selected rivers for GCM validation', *Techical Report 100, Max-Planck-Institut fur Meteorologie* .

Evensen, G. (1998), 'A Circulation Model for the West African Coast: Current Simulations for the WAX Project.', *Technical Report No. 154, NERSC* p. 36.

Evensen, G., Haugen, V. & Szabo, D. (2002), 'WANE Current Simulation Techinal Summary.', *Technical Note, NERSC* p. 18.

Florenchie, P., Lutjeharms, J., Reason, C., Masson, S. & Rouault, M. (2003), 'The Source of Benguela Niños in the South Atlantic Ocean.', *Geophysical Research Letters* **30, No10**.

Gammelsrød, T., Bartholomae, C., Boyer, D., Filipe, V. & O'Toole, M. (1998), 'Intrusion of Warm Surface Water along the Angolan-Namibian Coast in February-March 1995: the 1995 Benguela Nino.', *South African Journal of Marine Science* **19**, 41–56.

Halliwell, G. (2001), 'HYCOM Overview.', *Available online on the HYCOM Homepage: http://oceanmodeling.rsmas.miami.edu/hycom/* .

Halliwell, G. (2002), 'An Overview of HYCOM.', *Availabel online on the HYCOM Homepage: http://oceanmodeling.rsmas.miami.edu/hycom/* .

Kvaleberg, E. (2000), 'The 1995 Benguela Niño by means of remote sensing', *Cand. Scient. thesis, Geophysical Institute, University of Bergen* .

Lass, H., Schmidt, M., Mohrholz, V. & Nausch, G. (2000), 'Hydrographic and Current Measurements in the Area of the Angola-Benguela front.', *Journal of physical oceanography* **30**, 2589–2609.

Madec, G., Delecluse, P., Imbard, M. & Levy, C. (1998), 'OPA 8.1 Ocean General Circulation Model reference manual', *Internal report number XX, Institut Pierre Simon Laplace, Paris* .

Meeuwis, J. & Lutjeharms, J. (1990), 'Surface thermal characteristics of the Angola-Benguela front', *South African Journal of Marine Science* **9**, 261–279.

Mohrholz, V., Schmidt, M. & Lutjeharms, J. (2001), 'The hydrography and dynamics of the Angola-Benguela Frontal Zone and environment in April 1999.', *South African Journal of Marine Science* **97**, 199–208.

O'Toole, M. (1980), 'Seasonal distribution of temperature and salinity in the surface waters off south west Africa, 1972-1974.', *Investigational Report South Africa Sea Fisheries Institute* **121**, 1–25.

Peterson, R. & Stramma, L. (1991), 'Upper-level circulation in the South Atlantic Ocean', *Progress in Oceanography* **26**, 1–73.

Reynolds, R. & Smith, T. (1994), 'Improved global sea surface temperature analyses using optimum interpolation', *Journal of Climate* **7**, 929–948.

Rouault, M., Florenchie, P., Fauchereau, N. & Reason, C. (2003), 'South East tropical Atlantic warm events and southern African reainfall', *Geophysical Research Letters* **30, No5**.

Shannon, L., Brundrit, G., Taunton-Clark, J. & Boyd, A. (1986), 'On the existence of an El Niño-type phenomenon in the Benguela System', *Journal of marine research* **44**, 495–520.

Shannon, L. & Nelson, G. (1996), 'The Benguela: Large Scale Features and Processes and System Variability.', *Wefer, G., Berger, W.H., Sidler, G. and D.J. Webb: The South Atlantic: Present and Past Circulation.* **Berlin; Springer**, 163–210.

Tomczak, M. & Godfrey, J. (2003), *Regional Oceangraphy: an Introduction*, Daya Publishing House.